

1 **Human Cytomegalovirus Immediate-Early 1 Protein Causes Loss of SOX2**
2 **from Neural Progenitor Cells by Trapping Unphosphorylated STAT3 in the**
3 **Nucleus**

4 Short title: IE1-STAT3 Mediates SOX2 Depletion from NPC

5

6 Cong-Cong Wu^{1,2}✉, Xuan Jiang³✉, Xian-Zhang Wang^{1,2}✉, Xi-Juan Liu¹, Xiao-Jun Li¹, Bo
7 Yang¹, Han-Qing Ye¹, Thomas Harwardt^{4†}, Man Jiang⁵, Hui-Min Xia³, Wei Wang⁶, William J.
8 Britt⁷, Christina Paulus^{4,8}, Michael Nevels^{8#}, Min-Hua Luo^{1,2,3#}

9

10 **1** State Key Laboratory of Virology, Chinese Academy of Sciences Center for Excellence in
11 Brain Science and Intelligence Technology, Wuhan Institute of Virology, Wuhan, China

12 **2** University of Chinese Academy of Sciences, Beijing, China

13 **3** Guangzhou Women and Children's Medical Center, Guangzhou Medical University,
14 Guangzhou, China

15 **4** Institute for Medical Microbiology and Hygiene, University of Regensburg, Regensburg,
16 Germany

17 **5** Department of Physiology, School of Basic Medicine and Tongji Medical College,
18 Huazhong University of Science and Technology, Wuhan, China.

19 **6** The Third Xiangya Hospital, Central South University, Changsha, China

20 **7** Department of Pediatrics, University of Alabama School of Medicine, Birmingham,
21 Alabama, USA

22 **8** Biomedical Sciences Research Complex, University of St Andrews, St Andrews, United
23 Kingdom

24

25 ✉ CCW, XJ and XZW contributed equally to this work

26 † Deceased

27 # Address correspondence to luomh@wh.iov.cn (MHL) or mmn3@st-andrews.ac.uk (MN)

28 **ABSTRACT (141 words)**

29

30 The mechanisms underlying neurodevelopmental damage caused by virus infections remain
31 poorly defined. Congenital human cytomegalovirus (HCMV) infection is the leading cause of
32 fetal brain development disorders. Previous work has linked HCMV to perturbations of neural
33 cell fate, including premature differentiation of neural progenitor cells (NPCs). Here we show
34 that HCMV infection of NPCs results in the loss of the SOX2 protein, a key pluripotency-
35 associated transcription factor. SOX2 depletion maps to the HCMV major immediate-early
36 (IE) transcription unit and is individually mediated by the IE1 and IE2 proteins. IE1 causes
37 SOX2 down-regulation by promoting the nuclear accumulation and inhibiting the
38 phosphorylation of STAT3, a transcriptional activator of SOX2 expression. Deranged
39 signaling resulting in depletion of a critical stem cell protein is an unanticipated mechanism
40 by which the viral major IE proteins may contribute to brain development disorders caused by
41 congenital HCMV infection.

42 **IMPORTANCE (110 words)**

43

44 Human cytomegalovirus (HCMV) infections are a leading cause of brain damage, hearing
45 loss and other neurological disabilities in children. We report that the HCMV proteins known
46 as IE1 and IE2 target expression of human SOX2, a central pluripotency-associated
47 transcription factor that governs neural progenitor cell (NPC) fate and is required for normal
48 brain development. Both during HCMV infection and when expressed alone, IE1 causes the
49 loss of SOX2 from NPCs. IE1 mediates SOX2 depletion by targeting STAT3, a critical
50 upstream regulator of SOX2 expression. Our findings reveal an unanticipated mechanism by
51 which a common virus may cause damage to the developing nervous system and suggest
52 novel targets for medical intervention.

53 INTRODUCTION

54

55 Congenital human cytomegalovirus (HCMV) infection is the leading cause of birth defects
56 worldwide. Approximately 1% of live newborns are infected *in utero* with this virus. At the
57 time of birth, 5 to 10% of HCMV-infected newborn infants will exhibit signs of neurological
58 damage, such as microcephaly, cerebral calcification and other abnormal findings (1-3).
59 Among infected newborns that have no symptoms at birth, 10 to 15% subsequently develop
60 central nervous system (CNS) disorders, including sensorineural hearing loss, mental
61 retardation and learning disability (4-6). In addition, some authors have suggested that autism,
62 language disorders and other more subtle changes in brain development might be related to
63 congenital HCMV infection (7-9).

64 Although this virus can infect a wide range of organs *in vivo*, the fetal brain is regarded
65 the principal target of HCMV infection that results in neurological manifestations (10-12).
66 Due to exquisite host-specific tropism of this virus and the lack of animal models that
67 faithfully recapitulate major characteristics of human infection, the pathogenesis of HCMV-
68 associated disease in the developing CNS is largely unknown. However, recent advances in
69 human neural progenitor cell (NPC) isolation and culture have provided an opportunity to
70 study HCMV infection in a cell system relevant to fetal neuropathogenesis. Our previous
71 studies and the work of others have shown that human NPCs are susceptible to HCMV
72 infection and fully permissive to viral replication (13-19). HCMV infection of NPCs affects
73 the cell fate by causing premature differentiation (14, 17, 18). Whole-genome analysis
74 demonstrated that HCMV infection modulates the expression of NPC markers (14, 19)
75 including sex-determining region Y (SRY)-box 2 (SOX2), a core transcriptional factor for
76 stem cell self-renewal and pluripotency.

77 SOX2 is widely expressed in early neuroectoderm and neural progenitor cells during
78 development (14, 19, 20) as well as in neural stem cells in the adult brain (20, 21). SOX2
79 missense or heterozygous loss-of-function mutations have been identified to cause ocular
80 malformations, often manifesting as anophthalmia, microphthalmia, or coloboma. These
81 symptoms may be accompanied by hearing loss, learning disability, or brain malformation
82 (22-24). Familial recurrence of SOX2-associated anophthalmia has been observed (24).
83 Moreover, the level of SOX2 expression plays an important role in sensory organ, including
84 inner ear and retina, development. Groundbreaking research has demonstrated that forced
85 SOX2 expression in fibroblasts, with or without additional factors, can generate induced
86 pluripotent stem cells (25-27). In fact, ectopic SOX2 expression directs reprogramming of
87 fibroblasts into neural stem or precursor cells (25, 28-30). SOX2 is also critical for
88 maintenance of embryonic stem cells (ESCs). The SOX2 levels in ESCs are tightly regulated
89 (31) and even small changes in expression can lead to differentiation (32, 33).

90 STAT3 is a member of the signal transducer and activator of transcription family (34)
91 and is expressed in an activated form in the developing CNS as early as during initial NPC
92 proliferation. This protein plays a dichotomous regulatory role in neuro- and gliogenesis (35,
93 36). STAT3 is activated through phosphorylation of tyrosine 705 (Y705) by receptor-
94 associated kinases in response to various growth factors and cytokines including interleukin 6
95 (IL-6). Tyrosine phosphorylation leads to the nuclear accumulation of STAT3 homodimers,
96 which act as DNA binding transcriptional activators of numerous target genes including
97 SOX2. In ESCs that are differentiated into NPCs, STAT3 promotes cell fate commitment by
98 activating the SOX2 promoter (37).

99 Here we investigate the effects of HCMV infection on SOX2 expression in human
100 NPCs. We demonstrate that the HCMV 72-kDa immediate-early 1 (IE1) protein down-
101 regulates SOX2 transcription and mediates depletion of the SOX2 protein from HCMV-

102 infected NPCs. IE1 exerts its effect on SOX2 expression by inactivating the upstream
103 regulator STAT3.

104 **RESULTS**

105

106 **HCMV infection of NPCs causes down-regulation of SOX2 mRNA and protein.** Previous
107 work has established that human NPCs are fully permissive to HCMV infection (15, 38). As
108 early as 4 h post infection (hpi), a significant decrease of SOX2 mRNA was observed in
109 NPCs, and this decrease became more apparent as infection progressed (Fig 1A). In contrast,
110 SOX2 protein levels did not change in these cells at early post-infection times (up to 12 hpi),
111 but a gradual decrease was observed at late times (from 24 hpi) compared with mock-infected
112 cells (Fig 1B). By 48 hpi, the SOX2 protein was clearly down-regulated, and by 96 hpi it was
113 undetectable. The HCMV proteins IE1/IE2, UL44 and gB were also analyzed in this
114 experiment to monitor IE, early, and late viral gene expression, respectively.

115 In addition, the change in SOX2 protein levels was examined in relation to the
116 formation and development of HCMV intranuclear replication compartments visualized via
117 immunofluorescence staining of UL44 (Fig 1C). UL44 is the processivity factor of the
118 HCMV DNA polymerase and is first expressed in the early phase of infection. Initially, UL44
119 was evenly distributed across the infected nucleus, then it formed multiple small foci (36 hpi)
120 representing early viral replication compartments, and finally the small foci merged into
121 bipolar foci (48 hpi) or single large late replication compartments (72 hpi, data not shown). In
122 mock-infected NPCs, SOX2 exhibited its typical intense and diffuse nuclear staining. As
123 expected, the SOX2 signal decreased during the course of HCMV infection inversely relating
124 to UL44 foci development. In fact, SOX2 became dispersed and largely disappeared from late
125 HCMV-infected NPCs.

126 These observations indicate the presence of a highly effective mechanism for SOX2
127 depletion in HCMV-infected NPCs.

128

129 **SOX2 depletion from HCMV-infected NPCs requires *de novo* viral protein synthesis.** To
130 determine if SOX2 down-regulation is dependent on HCMV gene products expressed *de novo*
131 from the infecting viral genome, NPCs were exposed to infectious HCMV or UV-inactivated
132 virus and SOX2 expression was analyzed. As expected, SOX2 expression was suppressed at
133 both the RNA and protein level in infections with the untreated virus (Fig 2A and 2B). In
134 contrast, UV-inactivated virus failed to suppress the expression of SOX2 mRNA (Fig 2A) and
135 protein (Fig 2B). Similar levels of glycoprotein B (gB) derived from the input virus were
136 detected at 12 hpi with both untreated and UV-treated HCMV, confirming that cells had been
137 exposed to equal amounts of infecting virus (Fig 2B). However, *de novo* synthesis of viral
138 proteins was undetectable in infections with UV-treated virus confirming successful
139 inactivation. In another experiment, NPCs were pretreated with cycloheximide (CHX) and
140 then infected with HCMV for 16 h in the presence of CHX. Down-regulation of SOX2
141 mRNA induced by HCMV infection was significantly diminished by CHX treatment (Fig
142 2C). No obvious change in SOX2 protein levels was observed by 16 hpi (data not shown),
143 consistent with the results from Fig 1 and previous reports [14, 19].

144 These results indicate that one or more viral proteins expressed *de novo* upon HCMV
145 infection are required for SOX2 down-regulation in NPCs.

146

147 **HCMV major IE proteins mediate SOX2 down-regulation in NPCs.** Transcription of
148 SOX2 is suppressed as early as 4 hpi, a time when virion constituents and IE gene products
149 are the only viral components present in the infected cell nucleus. To test whether IE or
150 tegument proteins are sufficient for SOX2 down-regulation, the major IE proteins (IE1 and
151 IE2) and the most abundant tegument protein (pp65) were individually expressed in NPCs
152 using nucleofection. In agreement with the conclusion that newly synthesized viral proteins
153 mediate SOX2 down-regulation (Fig 2), SOX2 levels did not change in NPCs transiently

154 expressing pp65 compared to control cells (Fig 3A). Thus, pp65 was used as a negative
155 control in subsequent assays. Expression of the entire major IE transcription unit, including
156 the IE1 and IE2 proteins, resulted in significant reduction of SOX2 protein levels (Fig 3A). To
157 discriminate between effects on SOX2 expression mediated by IE1 or IE2, each of the two
158 proteins was individually expressed in NPCs. Following transfection of 2 or 5 μ g IE1
159 expressing plasmid, the relative SOX2 mRNA levels were reduced to 61 or 23% of control
160 levels, and the corresponding protein levels were reduced to 84 or 33%, respectively (Fig 3B).
161 Transfection of 2 or 5 μ g IE2 expressing plasmid reduced the relative SOX2 mRNA levels to
162 71 or 31% of control levels and the protein levels to 88 or 54%, respectively (Fig 3C).

163 These results indicate that the HCMV IE1 and IE2 proteins both play a significant role
164 in down-regulating SOX2 expression. However, IE1 appeared to affect SOX2 more efficiently
165 than IE2. Therefore, and because of the lethal phenotype of IE2-deficient viruses (39, 40), we
166 focused our study on the role of IE1 in SOX2 regulation in present study.

167

168 **HCMV IE1 is required for depletion of SOX2 during infection of NPCs.** HCMV infection
169 and IE1 expression were each sufficient to efficiently down-regulate SOX2 at the mRNA and
170 protein level in NPCs. To confirm the requirement of IE1 for SOX2 depletion during HCMV
171 infection, the expression of IE1 was knocked down using shRNAs targeting IE1 exon 4
172 sequences. First, human embryonic lung (HEL) cells were transduced with lentiviruses
173 expressing shRNAs directed against three different IE1-specific sequences, sh-1 to -3, or a
174 scrambled shRNA control (scr). The transduced cells were subsequently synchronized and
175 infected with HCMV. Analysis of IE1 protein levels determined at 24 and 48 hpi showed that
176 sh-2 was the most efficient among the three tested shRNAs in reducing the levels of the IE1
177 protein (Fig 4A). To confirm the knock-down efficiency of sh-2, another experiment was
178 performed where both IE1 mRNA and protein were analyzed at 24, 48 and 72 hpi. Again, sh-2

179 knocked down IE1 by >60% at the RNA level and 50% at the protein level through the course
180 of infection (Fig 4B).

181 Following the successful IE1 knock-down in HEL cells, NPCs were transduced with
182 lentiviruses expressing sh-2 or scr. The transduced NPCs were infected with HCMV and
183 collected at 24 to 60 hpi. Since 24 hpi was previously shown to be the “turning point” of
184 SOX2 protein levels (Fig 1), this time point was chosen as the earliest. As shown in Fig 4C,
185 SOX2 protein levels gradually decreased as infection progressed, consistent with Fig 1.
186 Significant knock-down of IE1 was observed at all tested time points in NPCs expressing sh-2
187 compared with scr expressing cells. SOX2 down-regulation was alleviated in HCMV-infected
188 NPCs expressing sh-2 compared to cells expressing scr, most notably at 60 hpi.

189 Although the IE1 knock-down was incomplete and linked to reduced levels of other
190 viral proteins (UL44 and gB), these results support the idea that IE1 contributes to SOX2
191 down-regulation during HCMV infection of NPCs.

192

193 **HCMV infection and IE1 expression inhibit STAT3 tyrosine phosphorylation and**
194 **relocalize unphosphorylated STAT3 to the nuclei of NPCs.** So far, our experiments have
195 indicated that HCMV IE1 down-regulates SOX2, but a mechanism through which the viral
196 protein alters expression of the cellular stem cell factor has not been identified. Results from
197 co-immunoprecipitation and yeast two hybrid assays failed to provide evidence for a physical
198 interaction between IE1 and SOX2 (data not shown). Since SOX2 expression was affected at
199 both the protein and RNA level, it also seemed more likely that IE1 interferes with
200 transcription rather than protein stability of SOX2. One key transcription factor regulating
201 SOX2 expression is STAT3 (37), which has been recently identified as a physical interaction
202 partner of IE1 (41, 42).

203 To investigate whether HCMV infection and IE1 expression affect SOX2 levels via

204 modulation of STAT3 activation, the levels of total and tyrosine (Y705)-phosphorylated
205 STAT3 (pSTAT3) were determined in infected NPCs. HCMV infection dramatically
206 suppressed STAT3 tyrosine phosphorylation as early as 4 hpi, and pSTAT3 was maintained at
207 low levels throughout the course of infection as compared to mock-infected NPCs. In
208 contrast, the total STAT3 levels showed little if any changes during infection (Fig 5A).

209 STAT3 is a nucleocytoplasmic shuttling protein which is efficiently exported from the
210 nucleus in its unphosphorylated form (43). Unphosphorylated STAT3 is therefore typically
211 located in the cytoplasm or distributed across both the nuclear and cytoplasmic compartments.
212 However, upon tyrosine phosphorylation pSTAT3 efficiently accumulates in the nucleus (37,
213 44, 45). To define the subcellular distribution of STAT3 in HCMV-infected NPCs, we
214 performed immunofluorescence analysis. NPCs on coverslips were infected with HCMV
215 (MOI=1), collected at 8 hpi, and stained for STAT3 and IE1/IE2. STAT3 was mainly confined
216 to the nuclei of virus-infected cells, while in mock-infected cells the STAT3 signal was more
217 diffuse and cytoplasmic as well as nuclear (Fig 5B). This observation was consistent with our
218 results from HCMV-infected fibroblasts (41, 42). To further investigate STAT3 subcellular
219 localization in HCMV-infected NPCs, the levels of pSTAT3 and total STAT3 in cytoplasmic
220 and nuclear compartments separated by cellular fractionation were analyzed at 4 and 8 hpi.
221 GAPDH and lamin B1 served as loading controls for the cytoplasmic and nuclear
222 compartments, respectively, confirming successful fractionation. As expected, pSTAT3 was
223 present predominantly in the nucleus of both mock- and HCMV-infected cells. Compared to
224 mock-infected NPCs, pSTAT3 levels were reduced in both the cytoplasm and nucleus of
225 HCMV-infected cells at 4 and 8 hpi. Total STAT3 resided mainly in the cytoplasm, but the
226 nuclear signal was much stronger in HCMV-infected compared with mock-infected cells at
227 both tested time points (Fig 5B). These results indicate that HCMV infection reduces the
228 levels of activated STAT3 (pSTAT3) and promotes the nuclear accumulation of

229 unphosphorylated STAT3 at very early times of infection in NPCs.

230 IE proteins are thought to be the only HCMV gene products expressed at 4 to 8 hpi,
231 when STAT3 is relocalized to the nucleus and its phosphorylation is inhibited. To test whether
232 IE1 was responsible for the observed effects on STAT3, the viral protein was transiently
233 expressed in NPCs. IE1 expression was sufficient to down-regulate pSTAT3 levels and to
234 sequester an unphosphorylated form of the cellular protein in the nuclear compartment (Fig
235 5C). To further confirm the role of IE1 in altering STAT3 phosphorylation and intracellular
236 localization, NPCs were mock-infected or infected with WT, dlIE1, or rvIE1 viruses. The
237 levels of viral proteins (UL44, gB) were similar, except that IE1 was absent and down-
238 regulation of SOX2 was diminished in the infection with dlIE1 (Fig 5D). Compared with
239 mock-infected cells, the pSTAT3 levels were reduced in WT- and rvIE1-, but not in dlIE1-
240 infected cells. Again, the overall steady-state STAT3 levels were rather constant across all
241 mock- and HCMV-infected samples (Fig 5E). Finally, based on cellular fractionation analysis,
242 pSTAT3 was located in the nuclei of both mock- and WT- or dlIE1-infected cells. Total
243 STAT3 localized mainly in the cytoplasm of mock- and dlIE1-infected cells, while increased
244 nuclear localization was observed in WT-infected NPCs (Fig 5F).

245 These results demonstrate that IE1 is both sufficient and required for the inhibition of
246 tyrosine phosphorylation and nuclear sequestration of unphosphorylated STAT3 observed
247 during HCMV infection of NPCs.

248

249 **SOX2 down-regulation in HCMV-infected NPCs results from IE1-mediated inhibition of**
250 **STAT3 activation.** The results thus far obtained are all consistent with a mechanism in which
251 IE1 mediates SOX2 down-regulation by limiting STAT3 activation. To further test this
252 possibility, we performed several different experiments. We first treated NPCs with CTS, a
253 chemical inhibitor of STAT3 tyrosine phosphorylation (46). In the presence of CTS, pSTAT3

254 levels (but not steady-state STAT3 levels) markedly decreased as a function of time of
255 treatment coinciding with gradual loss of SOX2 (Fig 6A). Then, STAT3 expression was
256 silenced using RNA interference. Two different shRNAs, shSTAT3-1 and shSTAT3-2,
257 knocked down STAT3 expression with different efficiencies compared to non-specific
258 shRNAs (shLuci and shDsRed). The extent of STAT3 silencing correlated with differential
259 reduction in pSTAT3 levels, in turn correlating with the levels of SOX2 (Fig 6B).

260 In addition to the experiments involving inhibition of STAT3, we set out to study the
261 IE1-STAT3-SOX2 axis by activating STAT3 signaling. To this end, we first treated NPCs with
262 IL-6, a major agonist of STAT3 signaling (47). IL-6 treatment led to a marked increase in
263 pSTAT3 without significantly affecting the overall STAT3 protein levels. Concurrent with
264 increased STAT3 tyrosine phosphorylation, there was also a rise in SOX2 levels. These data
265 were consistent with the finding that pSTAT3 promotes SOX2 expression in NPCs (Fig 6C).
266 Next, we transiently expressed IE1 in NPCs, treated the cells with IL-6 for 4 h or left them
267 untreated, and analyzed the levels of IE1, pSTAT3, total STAT3 and SOX2. Both pSTAT3 and
268 SOX2 were strongly up-regulated by IL-6, but down-regulated by IE1, and IL-6 efficiently
269 counteracted IE1-mediated down-regulation of pSTAT3 and SOX2. Again, the total steady-
270 state STAT3 levels did not significantly change upon IL-6 treatment or IE1 expression (Fig
271 6D). Finally, to further investigate the link between IE1 expression, STAT3 activation and
272 SOX2 regulation in the context of HCMV infection, NPCs were mock-infected or infected
273 with HCMV WT or dlIE1. The infected NPCs were treated with IL-6 for 4 h or left untreated
274 prior to collection at 24 and 48 hpi. As expected, IL-6 treatment led to elevated levels of
275 pSTAT3 and SOX2 in mock-, WT- and dlIE1-infected NPCs. HCMV WT infection reduced
276 the pSTAT3 levels slightly at 24 hpi and dramatically at 48 hpi. In contrast, no obvious
277 decrease of pSTAT3 was observed following dlIE1 infection. Concordantly, SOX2 protein
278 levels fell substantially in WT infection at 48 hpi, but remained constant in dlIE1 infection at

279 the same time point. Again, IL-6 treatment counteracted IE1-dependent down-regulation of
280 both pSTAT3 and SOX2 (Fig 6E).

281 In summary, these data demonstrate that SOX2 expression in NPCs strictly depends on
282 pSTAT3, and that there is a causal link between SOX2 down-regulation by HCMV and
283 inhibition of STAT3 activation by IE1, including inhibition of tyrosine phosphorylation and
284 trapping unphosphorylated STAT3 in nuclear.

285 **DISCUSSION**

286

287 Proliferation, differentiation and migration of NPCs as well as synapse formation among
288 mature neurons are all critical factors for fetal brain development and function (48-50).
289 HCMV infection has been shown to induce neural cell loss and abnormal differentiation of
290 NPCs (14, 15, 19). This was not only demonstrated *in vitro*, but also confirmed in a mouse
291 model of congenital infection where the virus appeared to affect NPCs in the subventricular
292 zone (12). Although HCMV is the leading cause of neurological damage in children, the
293 mechanisms by which the virus perturbs NPC proliferation and differentiation have remained
294 unclear.

295 SOX2 is a master controller of stem cells, strikingly illustrated by the fact that its
296 overexpression can reprogram terminally differentiated fibroblasts to induced pluripotent stem
297 cells (25-30). More specifically, SOX2 is a transcription factor essential for maintaining self-
298 renewal and pluripotency of ESCs and NPCs. SOX2 mutations cause symptoms resembling
299 damage resulting from congenital HCMV infection, including neural development disorders
300 accompanied by ocular malformation (22-24). In this study, we demonstrate that HCMV
301 significantly down-regulates SOX2 mRNA levels in human primary NPCs from as early as 4
302 hpi, extending our previous observations (14, 38). The reduced mRNA levels subsequently
303 lead to almost full depletion of the SOX2 protein from HCMV-infected cells at later times (24
304 to 96 hpi). The temporal delay between mRNA and protein down-regulation suggests that the
305 SOX2 protein may be very stable in NPCs, in contrast to what has been reported for ESCs
306 (51). The timing of changes in SOX2 mRNA levels and the observation that the down-
307 regulation depends on *de novo* viral protein synthesis, pointed us to the HCMV major IE
308 proteins as potential regulators of this stem cell factor. The 72-kDa IE1 and the 86-kDa IE2
309 protein subsequently proved to be sufficient to decrease SOX2 mRNA and protein levels in

310 the absence of other viral proteins, together and individually. IE1 and IE2 are nuclear
311 localized key regulators of viral and cellular transcription during infection (52-54). They have
312 been extensively studied in fibroblasts, but there is little information on how these proteins
313 behave in cell types more relevant to HCMV pathogenesis.

314 Our results demonstrate that the HCMV IE1 protein is not only sufficient, but also
315 necessary for the reduction of SOX2 levels through the early-late stages of infection. As noted
316 above, the down-regulation of SOX2 RNA and protein was also observed with ectopically
317 expressed HCMV IE2, but this protein appeared to be less efficient than IE1 in this respect.
318 We propose that IE2 also contributes to SOX2 down-regulation in the context of HCMV
319 infection, although this remains to be formally shown. Due to the difficulties in working with
320 IE2-deficient viruses (IE2 is essential for HCMV replication and difficult to complement), we
321 focused on IE1 in this study. Our findings may come as a surprise in the light of two previous
322 reports which concluded that HCMV infection or IE1 expression leads to increased instead of
323 decreased SOX2 levels in human glioma stem-like cells, human glioblastoma cells and mouse
324 glioma tissue (55, 56). The seemingly disparate findings might be due to differences in cell
325 types or virus strains. However, in our hands, IE1 induced robust inhibition of STAT3
326 activation in all cell types tested so far including glioblastoma-derived cell lines (data not
327 shown). Notably, the previous studies did not discriminate between the levels of SOX2 in IE1
328 expressing cells and IE1-negative cells in the same culture or tumor. Even if the STAT3
329 pathway is inhibited in HCMV-infected cells or cells ectopically expressing IE1, the
330 secretome associated with these cells may trigger STAT3 signaling in IE1-negative bystander
331 cells. In population analyses, this bystander effect may be detected as an overall increase in
332 STAT3-dependent gene expression (42).

333 Our work also determines the molecular events underlying IE1-dependent SOX2 down-
334 regulation, which appear to be intimately linked to JAK-STAT signaling. JAK-STAT (STAT1

335 and STAT3) signaling pathways play an important role in neural development by regulating
336 NPC neurogenesis and gliogenesis (35, 36). IE1 markedly affects the activation state and
337 subcellular localization of STAT3, a key regulatory protein known to affect the pluripotency
338 of ESCs and initiate the commitment to NPC fate via transcriptional activation of SOX2 (37).
339 IE1 inhibits tyrosine (Y705) phosphorylation and promotes nuclear accumulation of STAT3
340 without altering the protein's overall steady-state levels. These observations closely
341 recapitulate previous results in fibroblasts and are likely the consequence of a direct physical
342 interaction between IE1 and STAT3 (41, 42). Although paradoxical on the face of it,
343 decreased tyrosine phosphorylation and increased nuclear localization of STAT3 may be
344 coupled. STAT proteins, including STAT3, continually shuttle between the cytoplasm and the
345 nucleus. In fact, STAT3 is imported to the nucleus independent of tyrosine phosphorylation,
346 and this is normally followed by export to the cytoplasm. Tyrosine phosphorylation
347 transiently increases STAT3 nuclear accumulation due to sequestration by DNA binding or
348 heterodimerization with other phosphorylated STAT proteins (43). Likewise, IE1 may bind to
349 STAT3 passing through the nucleus. Nuclear sequestration may reduce the amounts of STAT3
350 undergoing export to the cytoplasm and, consequently, the pools of cytoplasmic STAT3
351 available for tyrosine phosphorylation by the corresponding (cytoplasmic) JAK family
352 kinases. The expected consequences of depleting activatable STAT3 by nuclear sequestration
353 are in line with the reduced pSTAT3 levels, restricted responsiveness to IL-6 and diminished
354 expression of SOX2 we observed in HCMV-infected NPCs.

355 In summary, this study initially links the interaction between IE1 and STAT3 to SOX2
356 depletion and thereby identifies a novel pathway predicted to contribute to developmental
357 neuropathogenesis caused by congenital HCMV infection.

358 **MATERIALS AND METHODS**

359 **Ethics statement.** Postmortem fetal brain tissues from different gestational age cases were
360 obtained according to the approval notice from the Institutional Review Board
361 (WIVH10201202) and the Guidelines for Biomedical Research Involving Human Subjects at
362 Wuhan Institute of Virology, Chinese Academy of Sciences. The original source of the
363 anonymized tissues was Zhongnan Hospital of Wuhan University (China). The cell isolation
364 procedures and research plans were approved by the Institutional Review Board (IRB)
365 (WIVH10201202) according to the Guidelines for Biomedical Research Involving Human
366 Subjects at Wuhan Institute of Virology, Chinese Academy of Sciences. The need for written
367 or oral consents was waived by IRB (57).

368

369 **Cells and cell culture**

370 All cells were maintained at 37°C in a humidified atmosphere containing 5% CO₂. NPCs
371 were isolated as described previously (38, 58) and cultured in a 1:1 mix of growth medium
372 and conditioned medium (14, 15, 19). The NPC growth medium was Dulbecco's Modified
373 Eagle Medium (DMEM)-F12 (Thermo Fisher Scientific) supplemented with 2 mM
374 GlutaMAX (Thermo Fisher Scientific), 100 U/ml penicillin and 100 µg/ml streptomycin
375 (Thermo Fisher Scientific), 50 µg/ml gentamycin (Sigma), 1.5 µg/ml amphotericin B
376 (Thermo Fisher Scientific), 10% BIT 9500 (Stem Cell Technologies), 20 ng/ml epidermal
377 growth factor (EGF, Prospec) and 20 ng/ml basic fibroblast growth factor (FGF, Prospec).
378 Conditioned medium was collected from cultured NPCs and stored at -20°C after cell debris
379 had been removed by centrifugation. NPCs were maintained as monolayers in fibronectin-
380 coated dishes and seeded at a defined density into dishes coated with poly-D-lysine (50 µg/ml,
381 Millipore) prior to infection. In order to induce STAT3 activation, NPCs were treated with
382 carrier-free recombinant human IL-6 (183 ng/ml, Biolegend) for the indicated times before

383 being collected for protein analysis. To inhibit STAT3 activation, NPCs were treated for the
384 indicated times with 10 μ M cryptotanshinone (CTS, Sigma), a small molecular inhibitor of
385 STAT3 tyrosine (Y705) phosphorylation.

386 Human embryonic lung fibroblasts (HEL cells, maintained in the laboratory) and HEL
387 cells immortalized by transfection with pCI-neo-hTERT (HELf cells, kindly provided by Dr.
388 Chen, Columbia University), were cultured in Minimal Essential Medium (MEM, Thermo
389 Fisher Scientific). Human embryonic kidney (HEK) 293T cells (CRL-11268) were grown in
390 DMEM. Both MEM and DMEM were supplemented with 10% fetal bovine serum (FBS,
391 Thermo Fisher Scientific), penicillin and streptomycin, and 2 mM L-glutamine (Thermo
392 Fisher Scientific). For the establishment of an IE1 expressing HELf cell line, a lentivirus
393 stock was prepared from plasmid pCDH-puro-IE1. A volume of 2 ml from this stock was used
394 to transduce 1×10^6 HELf cells. Transduced cells were cultured in normal medium for 2 days
395 to allow for transgene expression, and then switched to selection medium containing 8 μ g/ml
396 puromycin (Sigma) for 2 weeks with medium changes every other day. Expression of IE1 was
397 confirmed by Western blotting. The resulting HELf cell line stably expressing IE1 was
398 designated HELf-IE1 and maintained in medium containing puromycin (4 μ g/ml).

399

400 **Plasmids and nucleofection**

401 Plasmids pcDNA3-IE1 and pcDNA3-IE2 were constructed by subcloning a *Bam*HI-*Bam*HI
402 fragment containing the full-length coding sequence of the HCMV 72-kDa IE1 or 86-kDa IE2
403 protein, respectively, from pSG-IE1 or pSG-IE2 (kindly provided by Dr. Fortunato, University
404 of Idaho), respectively, into the backbone of pcDNA3.0. Plasmid pcDNA3-pp65 was
405 generated by cloning a fragment PCR-amplified from HCMV (Towne) cDNA between the
406 *Bam*HI and *Eco*RI sites of pcDNA3.0 (57). Plasmid pSVH (kindly provided by Dr. Tang,
407 Howard University) containing the entire HCMV major IE transcription unit (including IE1,

408 IE2 and the major IE promoter-enhancer) was also used.

409 Plasmids expressing short hairpin RNAs (shRNAs) directed against HCMV (Towne)
410 IE1 sequences were constructed based on lentiviral vector pLKO.1 puro (Addgene plasmid
411 #8453). Three shRNAs targeting IE1 exon 4 and a scrambled shRNA not targeting any viral
412 or human gene were designed (<http://jura.wi.mit.edu/bioc/siRNAext>), synthesized, and
413 inserted between the *AgeI* and *EcoRI* sites of pLKO.1 puro to generate pLKO.1-shRNA-IE1-1
414 (sh-1), pLKO.1-shRNA-IE1-2 (sh-2), pLKO.1-shRNA-IE1-3 (sh-3), and pLKO.1-scramble
415 (scr), respectively. Sequences are listed in Table 1. For the establishment of HELf-IE1 cells
416 (described above), a fragment containing the IE1 coding sequence was recovered from pSG-
417 IE1 and cloned into the *BamHI* site of pCDH-CMV-MCS-EF1-puro (System Biosciences).
418 The resulting construct was designated pCDH-puro-IE1.

419 Plasmids expressing shRNAs directed against human STAT3 sequences were
420 constructed based on lentiviral vector Tet-pLKO-puro (Addgene plasmid #21915). Two
421 shRNA plasmids targeting STAT3, Tet-pLKO-puro-shSTAT3-1 and Tet-pLKO-puro-
422 shSTAT3-2, were generated by inserting annealed oligonucleotides #1102 and #1103 or #1134
423 and #1135, respectively, between the *EcoRI* and *AgeI* sites of Tet-pLKO-puro. Likewise,
424 plasmids Tet-pLKO-puro-shLuci and Tet-pLKO-puro-shDsRed expressing shRNAs directed
425 against *Photinus* luciferase or *Discosoma* red fluorescent protein sequences, respectively, not
426 present in human cells were constructed by inserting annealed oligonucleotides #1098 and
427 #1099 or #1038 and #1039, respectively, between the *EcoRI* and *AgeI* sites of Tet-pLKO-
428 puro. Oligonucleotide sequences are listed in Table 1.

429 To transiently overexpress individual viral proteins, NPCs were transfected with
430 plasmids pSVH, pcDNA3-IE1, pcDNA3-IE2, pmaxGFP (provided by Lonza to assess
431 transfection efficiency), pcDNA3-pp65, or empty vector (pcDNA3.0) using Nucleofector
432 technology (Lonza) according to the manufacturer's instructions. In brief, 5×10^6 NPCs were

433 mixed with 100 μ l Mesenchymal Stem Cell (MSC) Nucleofector Solution (82 μ l Nucleofector
434 Solution with 18 μ l Supplement 1) and 5 μ g pSVH, pcDNA3-IE1, pcDNA3-IE2, pmaxGFP,
435 pcDNA3-pp65, or pcDNA3.0. The cell-DNA suspension was transferred to certified cuvettes,
436 which were inserted into a Nucleofector II, and program A-033 was applied. Immediately
437 following nucleofection, 500 μ l NPC growth medium was added to the cuvette, and the
438 sample was gently transferred to poly-D-lysine-coated dishes. After 24 h, the culture medium
439 was replaced, and cells were analyzed at 48 h post transfection.

440

441 **HCMV preparation and infection**

442 Enhanced green fluorescent protein (EGFP) expressing bacterial artificial chromosome-
443 derived wild-type (T-BAC, herein referred to as TNWT), IE1-deficient (TNdlIE1), and
444 revertant (TNrvIE1) variants of the HCMV Towne strain (ATCC-VR977) and the parental
445 virus HCMV Towne strain (ATCC-VR977) were used in this study. The construction of
446 TNdlIE1 and TNrvIE1 was described previously (59). The TNWT and TNrvIE1 viruses were
447 propagated in HEL cells and titrated by plaque assay as described previously (60, 61). The
448 TNdlIE1 mutant was propagated and titrated in HELf-IE1 cells. HCMV particles from
449 infected cell supernatants were concentrated by ultracentrifugation, after removing the cell
450 debris by high speed centrifugation, and resuspended in NPC growth medium to avoid any
451 potential undesired effects induced by components (including FBS) in the medium used for
452 virus preparation (61). UV-inactivated HCMV was prepared by exposure to 6000 J/cm² in a
453 CL-1000 Ultraviolet Crosslinker (UVP), sodium pyruvate was added to a final concentration
454 of 5 mM to prevent damage from free radicals induced by ultraviolet radiation (62).

455 For NPC infections, confluent cell monolayers on fibronectin-coated dishes were
456 dissociated using Accutase (Millipore), 3×10^6 cells were reseeded in poly-D-lysine-coated
457 100-mm dishes or uncoated dishes with poly-D-lysine-coated coverslips, and cells were

458 allowed to attach overnight. Cells were exposed to HCMV at the indicated multiplicities of
459 infection (MOIs). For the evaluation of IE1-directed shRNAs, NPCs or HEL cells were
460 infected with HCMV at an MOI of 1. To overcome the delay of infection process of TNdIE1,
461 MOI of 10 was used. After incubation for 3 h to allow for virus adsorption, the inoculum was
462 removed and cells were refed with fresh medium. Cells were collected and analyzed at the
463 indicated times post infection. To study infection in the absence of *de novo* protein synthesis,
464 NPCs were pretreated with 10 µg/ml cycloheximide (CHX, Sigma) for 1 h prior to infection,
465 infected with HCMV in the presence of CHX (10 µg/ml), and collected at 16 hpi for RNA and
466 protein analysis.

467

468 **Lentivirus preparation and transduction**

469 Stocks of replication-defective lentiviruses were prepared as described previously (57, 63).
470 Briefly, 1.5×10^6 HEK 293T cells were seeded in a 100-mm dish. On the next day, calcium
471 phosphate precipitation was applied to cotransfect the cells with packaging plasmids pML-
472 $\Delta 8.9$ (12 µg) and pVSV-G (8 µg) (System Biosciences) along with 15 µg of one of the
473 following expression plasmids: pCDH-puro-IE1, pLKO.1-scramble, pLKO.1-shRNA-IE1-1,
474 pLKO.1-shRNA-IE1-2, pLKO.1-shRNA-IE1-3, Tet-pLKO-puro-shDsRed, Tet-pLKO-puro-
475 shLuci, Tet-pLKO-puro-shSTAT3-1, or Tet-pLKO-puro-shSTAT3-2. Following a medium
476 change, the lentivirus containing supernatants were collected 72 h after transfection and stored
477 at -80°C.

478 The lentivirus stocks were used to transduce HEL cells, HELf cells, or NPCs. To this
479 end, 5×10^6 NPCs were seeded in fibronectin-coated dishes and infected with equal volumes (2
480 ml) of lentivirus stock on the following day. Lentivirus stock was added to the NPCs again on
481 the next day. The inoculum was replaced with fresh culture medium 3 h after each
482 transduction. Likewise, 5×10^5 HEL cells were infected with 2 ml lentivirus stock on the day

483 following seeding, and the inoculum was replaced with fresh culture medium 5 h after
484 infection. The transduced cells were cultured for 3 days to allow for transgene expression,
485 before they were subjected to HCMV infection and/or RNA or protein analysis. The
486 transduction procedure used to establish HELf-IE1 cells is described above.

487

488 **Gene silencing with shRNAs**

489 To determine the IE1-specific silencing efficiency, equal amounts of shRNA expressing
490 lentiviruses (sh-1, sh-2, sh-3, and scr) were used to transduce HEL cells in parallel. The
491 resulting HEL cells were cultured for 2 days to allow for shRNA expression, and this was
492 followed by 2 days serum starvation with serum free medium to synchronize the cells. The
493 synchronized cells were reseeded in 60-mm dishes (1×10^6 cells/dish), allowed to attach, and
494 infected with HCMV (MOI = 1). The infected cells were collected at 24 and 48 hpi, and the
495 levels of IE1 were determined by protein analysis. After selection of the most efficient shRNA
496 (sh-2), NPCs were transduced with sh-2 and scr lentiviruses in parallel. Transduced NPCs
497 were cultured for 48 h to allow for shRNA expression, reseeded in poly-D-lysine-coated
498 dishes (3×10^6 cells/dish), and infected with HCMV (MOI = 1) on the following day. Cells
499 were collected at the indicated times post infection and subjected to protein and RNA
500 analysis.

501 NPCs transduced with shRNA expressing lentiviruses Tet-pLKO-puro-shDsRed, Tet-
502 pLKO-puro-shLuci, Tet-pLKO-puro-shSTAT3-1, or Tet-pLKO-puro-shSTAT3-2 (described
503 above) were treated with 1 μ g/ml doxycycline hyclate (Dox, Aladdin) for 48 h, with a medium
504 change after 24 h, to induce shRNA expression. Cells were collected and analyzed at the
505 indicated times.

506

507 **Quantitative reverse transcriptase PCR (qRT-PCR)**

508 Transfected or infected NPCs were collected at the indicated times. Total RNA was isolated
509 using the RNAiso Plus reagent (Takara) followed by RNase-free DNase I treatment (Thermo
510 Fisher Scientific) to remove residual genomic DNA. Equal amounts (500 ng) of DNA-free
511 RNA were reverse transcribed using the PrimeScript RT Reagent Kit (Perfect Real Time;
512 Takara) according to the manufacturer's instructions. Then, qPCR was performed in a CFX96
513 Connect Real-Time PCR Detection System (Bio-Rad). Each 20- μ l qPCR reaction contained 2
514 μ l RT product, 10 μ l 2 \times iTaq Universal SYBR Green Supermix (Bio-Rad), and 200 nM
515 forward (F) and reverse (R) primers. Primer sequences are shown in Table 1. Amplification
516 was performed by denaturation at 95°C for 5 min, followed by 35 two-step cycles of 95°C for
517 10 s and 60°C for 30 s. Melting curve analysis was carried out at 95°C for 1 min, 55°C for 1
518 min, and 55 to 95°C for 10 s. Each reaction was performed in triplicate, and results for the
519 target gene mRNA were normalized to glyceraldehyde 3-phosphate dehydrogenase (GAPDH)
520 using the $2^{-\Delta\Delta CT}$ method. Three independent experiments were performed, and results are
521 presented as the means \pm one standard deviation (SD). Data were statistically evaluated using
522 the Student's t-test. A *P*-value of ≤ 0.05 was considered statistically significant.

523

524 **Western blotting**

525 At the indicated times, cells were washed in phosphate-buffered saline (PBS), detached with
526 Accutase, collected, counted, and centrifuged. Cell pellets were snap-frozen in liquid nitrogen
527 and stored at -80°C until completion of the time course. Then, cell pellets were lysed in
528 radioimmunoprecipitation assay (RIPA) buffer. Equal amounts of cell lysates were separated
529 by sodium dodecyl sulfate-polyacrylamide gel electrophoresis (SDS-PAGE) and transferred to
530 polyvinylidene fluoride (PVDF) membrane (Millipore). After incubation with the indicated
531 primary and corresponding secondary antibodies, signals were detected using a
532 Chemiluminescence machine, and analyzed by densitometry program (Image J). At least three

533 sets of independent experiments were performed and representative results were shown.
534 HCMV proteins were detected using mouse monoclonal antibodies to IE1 (clone p63-27,
535 IgG2a), IE1/IE2 (CH16), UL44 (IgG1, Virusys), glycoprotein B (gB; clone 27-156, IgG2b),
536 or pp65 (IgG1, Virusys). Cellular proteins were detected using a goat polyclonal antibody to
537 SOX2 (clone L1D6A2, IgG1), a mouse monoclonal antibody to STAT3 (clone 124H6, IgG2a,
538 Cell Signaling Technology), a rabbit polyclonal antibody to pSTAT3 (Y705) (IgG, Cell
539 Signaling Technology), a mouse monoclonal antibody to β -actin (IgG, Santa Cruz
540 Biotechnology), a rabbit polyclonal antibody to GAPDH (IgG, Proteintech), or a rabbit
541 polyclonal antibody to lamin B1 (IgG, Proteintech). Secondary antibodies used were
542 horseradish peroxidase-conjugated sheep anti-mouse IgG (Amersham Bioscience), donkey
543 anti-rabbit IgG (Amersham Bioscience), or donkey anti-goat IgG (Proteintech).

544

545 **Immunofluorescence assay**

546 Viral and cellular proteins in cells grown on coverslips were detected by indirect
547 immunofluorescence analysis as described previously (64). Briefly, NPCs were seeded on
548 poly-D-lysine-coated coverslips in uncoated dishes and mock- or HCMV-infected (MOI = 3).
549 Coverslips were collected at the indicated times post infection. UL44, SOX2 or STAT3 were
550 stained with the respective primary antibodies: mouse monoclonal anti-UL44 (IgG1, Virusys),
551 goat polyclonal anti-SOX2 (Santa Cruz Biotechnology), or mouse monoclonal anti-STAT3
552 (clone 124H6, IgG2a, Cell Signaling Technology). The secondary antibodies included
553 fluorescein-isothiocyanate (FITC)-conjugated donkey anti-goat IgG (Jackson
554 Immunoresearch), Alexa Fluor 488-conjugated goat anti-mouse IgG1 (Molecular Probes), and
555 Alexa Fluor 488-conjugated goat anti-mouse IgG2a (Molecular Probes). Nuclei were
556 counterstained with Hoechst 33342 dye, and coverslips were mounted with anti-fade
557 mounting solution containing paraphenylenediamine (65). Images were obtained using a

558 Nikon Eclipse 80i or Nikon Eclipse Ti-S epifluorescence microscope equipped with a Nikon
559 DS-Ri1 camera and processed using the NIS-Elements F3.0 software.

560

561 **Cellular fractionation**

562 Nucleofected or infected NPCs were washed in pre-cooled PBS and collected by scraping.
563 Cytosolic and nuclear fractions were prepared using the Nuclear-Cytosol Extraction Kit
564 (Applygen Technologies) following the manufacturer's instructions. Briefly, cell pellets were
565 lysed in pre-cooled Cytosol Extraction Buffer A (CEB-A), vortexed, reacted with Cytosol
566 Extraction Buffer B (CEB-B), vortexed, and centrifuged. The resulting supernatant contained
567 the cytosolic fraction. The precipitate was washed with CEB-A, lysed in Nuclear Extraction
568 Buffer (NEB), vortexed, and centrifuged. The resulting supernatant contained the nuclear
569 fraction.

570 **ACKNOWLEDGMENTS**

571

572 We appreciate the critical reading from Tom Shenk. We thank the colleagues mentioned in
573 Materials and Methods for providing important reagents. MHL was supported by the Ministry
574 of Science and Technology of China (National Program on Key Basic Research Project
575 2015CB755600), the National Natural Science Foundation of China (81620108021,
576 31170155, and 81427801), the Sino-Africa Joint Research Centre (SAJC201605) and a seed
577 grant from the University of Idaho (YDP-764). MN and CP were supported by the Wellcome
578 Trust Institutional Strategic Support Fund, MN was supported by the Medical Research
579 Council (MR/P022146/1) and Tenovus Scotland (T15/38), and CP was supported by the
580 Deutsche Forschungsgemeinschaft (PA 815/2-1).

581 **REFERENCES**

- 582 1. **Bale JF, Jr.** 1984. Human cytomegalovirus infection and disorders of the nervous system. *Arch Neurol*
583 **41**:310-320.
- 584 2. **Stagno S, Pass RF, Cloud G, Britt WJ, Henderson RE, Walton PD, Veren DA, Page F, Alford CA.**
585 1986. Primary cytomegalovirus infection in pregnancy. Incidence, transmission to fetus, and clinical
586 outcome. *JAMA* **256**:1904-1908.
- 587 3. **Bale JF, Jr.** 2014. Congenital cytomegalovirus infection. *Handb Clin Neurol* **123**:319-326.
- 588 4. **Conboy TJ, Pass RF, Stagno S, Britt WJ, Alford CA, McFarland CE, Boll TJ.** 1986. Intellectual
589 development in school-aged children with asymptomatic congenital cytomegalovirus infection.
590 *Pediatrics* **77**:801-806.
- 591 5. **Pass RF, Stagno S, Myers GJ, Alford CA.** 1980. Outcome of symptomatic congenital
592 cytomegalovirus infection: results of long-term longitudinal follow-up. *Pediatrics* **66**:758-762.
- 593 6. **Rosenthal LS, Fowler KB, Boppana SB, Britt WJ, Pass RF, Schmid SD, Stagno S, Cannon MJ.**
594 2009. Cytomegalovirus shedding and delayed sensorineural hearing loss: results from longitudinal
595 follow-up of children with congenital infection. *Pediatr Infect Dis J* **28**:515-520.
- 596 7. **Sweeten TL, Posey DJ, McDougle CJ.** 2004. Brief report: autistic disorder in three children with
597 cytomegalovirus infection. *J Autism Dev Disord* **34**:583-586.
- 598 8. **Yamashita Y, Fujimoto C, Nakajima E, Isagai T, Matsuishi T.** 2003. Possible association between
599 congenital cytomegalovirus infection and autistic disorder. *J Autism Dev Disord* **33**:455-459.
- 600 9. **Zhang XW, Li F, Yu XW, Shi XW, Shi J, Zhang JP.** 2007. Physical and intellectual development in
601 children with asymptomatic congenital cytomegalovirus infection: a longitudinal cohort study in Qinba
602 mountain area, China. *J Clin Virol* **40**:180-185.
- 603 10. **Boppana SB, Pass RF, Britt WJ, Stagno S, Alford CA.** 1992. Symptomatic congenital
604 cytomegalovirus infection: neonatal morbidity and mortality. *Pediatr Infect Dis J* **11**:93-99.
- 605 11. **Dahle AJ, Fowler KB, Wright JD, Boppana SB, Britt WJ, Pass RF.** 2000. Longitudinal investigation
606 of hearing disorders in children with congenital cytomegalovirus. *J Am Acad Audiol* **11**:283-290.
- 607 12. **Tsutsui Y, Kosugi I, Kawasaki H.** 2005. Neuropathogenesis in cytomegalovirus infection: indication
608 of the mechanisms using mouse models. *Rev Med Virol* **15**:327-345.
- 609 13. **Cheeran MC, Hu S, Ni HT, Sheng W, Palmquist JM, Peterson PK, Lokensgard JR.** 2005. Neural
610 precursor cell susceptibility to human cytomegalovirus diverges along glial or neuronal differentiation
611 pathways. *J Neurosci Res* **82**:839-850.
- 612 14. **Luo MH, Hannemann H, Kulkarni AS, Schwartz PH, O'Dowd JM, Fortunato EA.** 2010. Human
613 cytomegalovirus infection causes premature and abnormal differentiation of human neural progenitor
614 cells. *J Virol* **84**:3528-3541.
- 615 15. **Luo MH, Schwartz PH, Fortunato EA.** 2008. Neonatal neural progenitor cells and their neuronal and
616 glial cell derivatives are fully permissive for human cytomegalovirus infection. *J Virol* **82**:9994-10007.
- 617 16. **McCarthy M, Auger D, Whittemore SR.** 2000. Human cytomegalovirus causes productive infection
618 and neuronal injury in differentiating fetal human central nervous system neuroepithelial precursor
619 cells. *J Hum Virol* **3**:215-228.
- 620 17. **Odeberg J, Wolmer N, Falci S, Westgren M, Seiger A, Soderberg-Naucler C.** 2006. Human
621 cytomegalovirus inhibits neuronal differentiation and induces apoptosis in human neural precursor cells.
622 *J Virol* **80**:8929-8939.
- 623 18. **Odeberg J, Wolmer N, Falci S, Westgren M, Sundtrom E, Seiger A, Soderberg-Naucler C.** 2007.
624 Late human cytomegalovirus (HCMV) proteins inhibit differentiation of human neural precursor cells
625 into astrocytes. *J Neurosci Res* **85**:583-593.
- 626 19. **Pan X, Li XJ, Liu XJ, Yuan H, Li JF, Duan YL, Ye HQ, Fu YR, Qiao GH, Wu CC, Yang B, Tian**
627 **XH, Hu KH, Miao LF, Chen XL, Zheng J, Rayner S, Schwartz PH, Britt WJ, Xu J, Luo MH.**
628 2013. Later passages of neural progenitor cells from neonatal brain are more permissive for human
629 cytomegalovirus infection. *J Virol* **87**:10968-10979.
- 630 20. **Wegner M.** 2011. SOX after SOX: SOXession regulates neurogenesis. *Genes Dev* **25**:2423-2428.
- 631 21. **Brazel CY, Limke TL, Osborne JK, Miura T, Cai J, Pevny L, Rao MS.** 2005. Sox2 expression
632 defines a heterogeneous population of neurosphere-forming cells in the adult murine brain. *Aging Cell*
633 **4**:197-207.
- 634 22. **Fantes J, Ragge NK, Lynch SA, McGill NI, Collin JR, Howard-Peebles PN, Hayward C, Vivian**
635 **AJ, Williamson K, van Heyningen V, FitzPatrick DR.** 2003. Mutations in SOX2 cause anophthalmia.
636 *Nat Genet* **33**:461-463.
- 637 23. **Ragge NK, Lorenz B, Schneider A, Bushby K, de Sanctis L, de Sanctis U, Salt A, Collin JR, Vivian**
638 **AJ, Free SL, Thompson P, Williamson KA, Sisodiya SM, van Heyningen V, Fitzpatrick DR.** 2005.
639 SOX2 anophthalmia syndrome. *Am J Med Genet A* **135**:1-7; discussion 8.

- 640 24. **Schneider A, Bardakjian TM, Zhou J, Hughes N, Keep R, Dorsainville D, Kherani F, Katowitz J,**
641 **Schimmenti LA, Hummel M, Fitzpatrick DR, Young TL.** 2008. Familial recurrence of SOX2
642 anophthalmia syndrome: phenotypically normal mother with two affected daughters. *Am J Med Genet*
643 *A* **146A**:2794-2798.
- 644 25. **Ring KL, Tong LM, Balestra ME, Javier R, Andrews-Zwilling Y, Li G, Walker D, Zhang WR,**
645 **Kreitzer AC, Huang Y.** 2012. Direct reprogramming of mouse and human fibroblasts into multipotent
646 neural stem cells with a single factor. *Cell Stem Cell* **11**:100-109.
- 647 26. **Takahashi K, Tanabe K, Ohnuki M, Narita M, Ichisaka T, Tomoda K, Yamanaka S.** 2007.
648 Induction of pluripotent stem cells from adult human fibroblasts by defined factors. *Cell* **131**:861-872.
- 649 27. **Takahashi K, Yamanaka S.** 2006. Induction of pluripotent stem cells from mouse embryonic and adult
650 fibroblast cultures by defined factors. *Cell* **126**:663-676.
- 651 28. **Kim J, Efe JA, Zhu S, Talantova M, Yuan X, Wang S, Lipton SA, Zhang K, Ding S.** 2011. Direct
652 reprogramming of mouse fibroblasts to neural progenitors. *Proc Natl Acad Sci U S A* **108**:7838-7843.
- 653 29. **Lujan E, Chanda S, Ahlenius H, Sudhof TC, Wernig M.** 2012. Direct conversion of mouse
654 fibroblasts to self-renewing, tripotent neural precursor cells. *Proc Natl Acad Sci U S A* **109**:2527-2532.
- 655 30. **Maucksch C, Firmin E, Butler-Munro C, Montgomery J, Dottori M, Connor B.** 2012. Non-Viral
656 Generation of Neural Precursor-like Cells from Adult Human Fibroblasts. *J Stem Cells Regen Med*
657 **8**:162-170.
- 658 31. **Rizzino A.** 2013. Concise review: The Sox2-Oct4 connection: critical players in a much larger
659 interdependent network integrated at multiple levels. *Stem Cells* **31**:1033-1039.
- 660 32. **Kopp JL, Ormsbee BD, Desler M, Rizzino A.** 2008. Small increases in the level of Sox2 trigger the
661 differentiation of mouse embryonic stem cells. *Stem Cells* **26**:903-911.
- 662 33. **Masui S, Nakatake Y, Toyooka Y, Shimosato D, Yagi R, Takahashi K, Okochi H, Okuda A,**
663 **Matoba R, Sharov AA, Ko MS, Niwa H.** 2007. Pluripotency governed by Sox2 via regulation of
664 Oct3/4 expression in mouse embryonic stem cells. *Nat Cell Biol* **9**:625-635.
- 665 34. **Imada K, Leonard WJ.** 2000. The Jak-STAT pathway. *Mol Immunol* **37**:1-11.
- 666 35. **Bonni A, Sun Y, Nadal-Vicens M, Bhatt A, Frank DA, Rozovsky I, Stahl N, Yancopoulos GD,**
667 **Greenberg ME.** 1997. Regulation of gliogenesis in the central nervous system by the JAK-STAT
668 signaling pathway. *Science* **278**:477-483.
- 669 36. **Sun Y, Nadal-Vicens M, Misono S, Lin MZ, Zubiaga A, Hua X, Fan G, Greenberg ME.** 2001.
670 Neurogenin promotes neurogenesis and inhibits glial differentiation by independent mechanisms. *Cell*
671 **104**:365-376.
- 672 37. **Foshay KM, Gallicano GI.** 2008. Regulation of Sox2 by STAT3 initiates commitment to the neural
673 precursor cell fate. *Stem Cells Dev* **17**:269-278.
- 674 38. **Pan W, Jin Y, Chen J, Rottier RJ, Steel KP, Kiernan AE.** 2013. Ectopic expression of activated
675 notch or SOX2 reveals similar and unique roles in the development of the sensory cell progenitors in
676 the mammalian inner ear. *J Neurosci* **33**:16146-16157.
- 677 39. **Heider JA, Bresnahan WA, Shenk TE.** 2002. Construction of a rationally designed human
678 cytomegalovirus variant encoding a temperature-sensitive immediate-early 2 protein. *Proc Natl Acad*
679 *Sci U S A* **99**:3141-3146.
- 680 40. **Marchini A, Liu H, Zhu H.** 2001. Human cytomegalovirus with IE-2 (UL122) deleted fails to express
681 early lytic genes. *J Virol* **75**:1870-1878.
- 682 41. **Reitsma JM, Sato H, Nevels M, Terhune SS, Paulus C.** 2013. Human cytomegalovirus IE1 protein
683 disrupts interleukin-6 signaling by sequestering STAT3 in the nucleus. *J Virol* **87**:10763-10776.
- 684 42. **Harwardt T, Lukas S, Zenger M, Reitberger T, Danzer D, Übner T, Munday DC, Nevels M,**
685 **Paulus C.** 2016. Human Cytomegalovirus Immediate-Early 1 Protein Rewires Upstream STAT3 to
686 Downstream STAT1 Signaling Switching an IL6-Type to an IFNgamma-Like Response. *PLoS Pathog*
687 **12**:e1005748.
- 688 43. **Reich NC.** 2013. STATs get their move on. *JAKSTAT* **2**:e27080.
- 689 44. **Fan G, Martinowich K, Chin MH, He F, Fouse SD, Hutnick L, Hattori D, Ge W, Shen Y, Wu H,**
690 **ten Hoeve J, Shuai K, Sun YE.** 2005. DNA methylation controls the timing of astroglialogenesis
691 through regulation of JAK-STAT signaling. *Development* **132**:3345-3356.
- 692 45. **Miller FD, Gauthier AS.** 2007. Timing is everything: making neurons versus glia in the developing
693 cortex. *Neuron* **54**:357-369.
- 694 46. **Shin DS, Kim HN, Shin KD, Yoon YJ, Kim SJ, Han DC, Kwon BM.** 2009. Cryptotanshinone
695 inhibits constitutive signal transducer and activator of transcription 3 function through blocking the
696 dimerization in DU145 prostate cancer cells. *Cancer Res* **69**:193-202.
- 697 47. **Onishi K, Zandstra PW.** 2015. LIF signaling in stem cells and development. *Development* **142**:2230-
698 2236.
- 699 48. **Biran J, Tahor M, Wircer E, Levkowitz G.** 2015. Role of developmental factors in hypothalamic

- 700 function. *Front Neuroanat* **9**:47.
- 701 49. **Guerrini R, Parrini E.** 2010. Neuronal migration disorders. *Neurobiol Dis* **38**:154-166.
- 702 50. **Hofman MA.** 2014. Evolution of the human brain: when bigger is better. *Front Neuroanat* **8**:15.
- 703 51. **Fang L, Zhang L, Wei W, Jin X, Wang P, Tong Y, Li J, Du JX, Wong J.** 2014. A methylation-
704 phosphorylation switch determines Sox2 stability and function in ESC maintenance or differentiation.
705 *Mol Cell* **55**:537-551.
- 706 52. **Noris E, Zannetti C, Demurtas A, Sinclair J, De Andrea M, Gariglio M, Landolfo S.** 2002. Cell
707 cycle arrest by human cytomegalovirus 86-kDa IE2 protein resembles premature senescence. *J Virol*
708 **76**:12135-12148.
- 709 53. **Spector DH.** 1996. Activation and regulation of human cytomegalovirus early genes. *Intervirology*
710 **39**:361-377.
- 711 54. **Stinski MF, Meier JL.** 2007. Immediate-early viral gene regulation and function. *In* Arvin A,
712 Campadelli-Fiume G, Mocarski E, Moore PS, Roizman B, Whitley R, Yamanishi K (ed.), *Human*
713 *Herpesviruses: Biology, Therapy, and Immunoprophylaxis*, Cambridge.
- 714 55. **Soroceanu L, Matlaf L, Khan S, Akhavan A, Singer E, Bezrookove V, Decker S, Ghanny S,**
715 **Hadacek P, Bengtsson H, Ohlfest J, Luciani-Torres MG, Harkins L, Perry A, Guo H,**
716 **Soteropoulos P, Cobbs CS.** 2015. Cytomegalovirus Immediate-Early Proteins Promote Stemness
717 Properties in Glioblastoma. *Cancer Res* **75**:3065-3076.
- 718 56. **Fornara O, Bartek J, Jr., Rahbar A, Odeberg J, Khan Z, Peredo I, Hamerlik P, Bartek J,**
719 **Stragliotto G, Landazuri N, Soderberg-Naucler C.** 2016. Cytomegalovirus infection induces a stem
720 cell phenotype in human primary glioblastoma cells: prognostic significance and biological impact. *Cell*
721 *Death Differ* **23**:261-269.
- 722 57. **Fu YR, Liu XJ, Li XJ, Shen ZZ, Yang B, Wu CC, Li JF, Miao LF, Ye HQ, Qiao GH, Rayner S,**
723 **Chavanas S, Davrinche C, Britt WJ, Tang Q, McVoy M, Mocarski E, Luo MH.** 2015. MicroRNA
724 miR-21 attenuates human cytomegalovirus replication in neural cells by targeting Cdc25a. *J Virol*
725 **89**:1070-1082.
- 726 58. **Schwartz PH, Bryant PJ, Fuja TJ, Su H, O'Dowd DK, Klassen H.** 2003. Isolation and
727 characterization of neural progenitor cells from post-mortem human cortex. *J Neurosci Res* **74**:838-851.
- 728 59. **Knoblach T, Grandel B, Seiler J, Nevels M, Paulus C.** 2011. Human cytomegalovirus IE1 protein
729 elicits a type II interferon-like host cell response that depends on activated STAT1 but not interferon-
730 gamma. *PLoS Pathog* **7**:e1002016.
- 731 60. **Shen ZZ, Pan X, Miao LF, Ye HQ, Chavanas S, Davrinche C, McVoy M, Luo MH.** 2014.
732 Comprehensive analysis of human cytomegalovirus microRNA expression during lytic and quiescent
733 infection. *PLoS One* **9**:e88531.
- 734 61. **Liu XJ, Yang B, Huang SN, Wu CC, Li XJ, Cheng S, Jiang X, Hu F, Ming YZ, Nevels M, Britt**
735 **WJ, Rayner S, Tang Q, Zeng WB, Zhao F, Luo MH.** 2017. Human cytomegalovirus IE1
736 downregulates Hes1 in neural progenitor cells as a potential E3 ubiquitin ligase. *PLoS Pathog*
737 **13**:e1006542.
- 738 62. **Fortunato EA, Dell'Aquila ML, Spector DH.** 2000. Specific chromosome 1 breaks induced by human
739 cytomegalovirus. *Proc Natl Acad Sci U S A* **97**:853-858.
- 740 63. **Tiscornia G, Singer O, Verma IM.** 2006. Production and purification of lentiviral vectors. *Nat Protoc*
741 **1**:241-245.
- 742 64. **Duan Y, Miao L, Ye H, Yang C, Fu B, Schwartz PH, Rayner S, Fortunato EA, Luo MH.** 2012. A
743 faster immunofluorescence assay for tracking infection progress of human cytomegalovirus. *Acta*
744 *Biochim Biophys Sin (Shanghai)* **44**:597-605.
- 745 65. **Luo MH, Rosenke K, Czornak K, Fortunato EA.** 2007. Human cytomegalovirus disrupts both ataxia
746 telangiectasia mutated protein (ATM)- and ATM-Rad3-related kinase-mediated DNA damage responses
747 during lytic infection. *J Virol* **81**:1934-1950.
- 748

749 **FIGURE LEGENDS**

750

751 **Figure 1. HCMV infection down-regulates SOX2 at the mRNA and protein level in**

752 **NPCs.** NPC monolayers were mock (M)- or virus (V)-infected with HCMV (TNWT) at an

753 MOI of 3 and collected at the indicated times post infection for mRNA or protein analyses.

754 (A) SOX2 mRNA levels during HCMV infection of NPCs. The levels of SOX2 mRNA

755 normalized to GAPDH were determined by qRT-PCR at 4 to 120 hpi. Log₁₀ values of virus-

756 to-mock (V/M) ratios are given for each time point. Results shown are average ± standard

757 deviation (SD) of data from three independent experiments, each conducted in triplicate. (B)

758 SOX2 and viral protein levels during HCMV infection of NPCs. SOX2, IE1/IE2, UL44, and

759 gB steady-state protein levels were determined by Western blotting at 4 to 96 hpi. Actin

760 served as a loading control. The values listed below the blots indicate the relative SOX2

761 protein levels compared to corresponding mock controls following actin normalization. ND,

762 not detectable. (C) Cellular distribution of SOX2 in relation to viral replication compartments

763 during HCMV infection of NPCs. The distributions of SOX2 and UL44 were determined by

764 indirect immunofluorescence assay at 12 to 48 hpi. NPCs grown on poly-D-lysine-coated

765 coverslips were stained with antibodies against SOX2 (green) and UL44 (red), nuclei were

766 counterstained with Hoechst 33342 (blue). Phase contrast images are also shown. Scale bars,

767 5 μm.

768

769 **Figure 2. *De novo* synthesis of HCMV proteins is required for SOX2 down-regulation in**

770 **NPCs.** Comparison of HCMV infections with active virus (V) and UV-inactivated virus

771 (UV). NPCs were mock-infected (M) or infected with active or UV-irradiated TNWT at an

772 MOI of 3 and collected at the indicated times post infection. (A) SOX2 mRNA levels

773 normalized to GAPDH were determined by qRT-PCR. Log₁₀ values of inactivated virus-to-

774 mock (UV/M) and active virus-to-mock (V/M) ratios are shown. Data from three independent
775 experiments were analyzed by one way ANOVA, and results are presented as average \pm SD.
776 **, $p \leq 0.01$. (B) Levels of SOX2 and representative viral proteins (IE1/IE2, UL44, and gB)
777 were determined by Western blotting. Actin served as a loading control. The values listed
778 below the blots indicate the relative SOX2 protein levels compared to corresponding
779 mock controls following actin normalization. Data were from three independent experiments,
780 results are presented as average \pm SD. *, $p \leq 0.05$; **, $p \leq 0.01$. (C) Effect of protein synthesis
781 inhibition by CHX treatment on SOX2 mRNA levels. NPCs were pretreated with CHX for 1 h
782 prior to infection, and then mock (M)- or virus (V)-infected with HCMV (TNWT) at an MOI
783 of 3. Cells were collected at 16 hpi for analysis of SOX2 mRNA by qRT-PCR. Data from
784 three independent experiments were analyzed by one way ANOVA, and results are presented
785 as average \pm SD. **, $p \leq 0.01$.

786

787 **Figure 3. HCMV major IE proteins down-regulate SOX2 mRNA and protein in NPCs.**

788 HCMV pp65, IE1, IE2 or IE1 and IE2 combined were transiently expressed in NPCs
789 following nucleofection. Samples were collected at 48 h post transfection for mRNA (qRT-
790 PCR) or protein (Western blotting) analysis. Actin served as a loading control. The relative
791 level of SOX2 protein compared to corresponding controls following actin normalization.
792 Data from three independent experiments were analyzed by one way ANOVA, and results are
793 presented as average \pm SD. *, $p < 0.05$; **, $p < 0.01$. (A) Effect of pp65 and major IE proteins
794 (IE1 and IE2) on SOX2 protein levels. Left: NPCs were transfected with 5 μ g pcDNA3.0
795 (vector) or pcDNA3-pp65. Right: NPCs were transfected with 5 μ g pcDNA3-pp65 as control
796 (vector) or pSVH (IE1 and IE2). (B) Effect of IE1 on SOX2 mRNA and protein levels. NPCs
797 were transfected with 5 μ g pcDNA3-pp65 (vector), or 2 to 5 μ g pcDNA3-IE1. (C) Effect of
798 IE2 on SOX2 mRNA and protein levels. NPCs were transfected with 5 μ g pcDNA3-pp65

799 (vector), or 2 to 5 μ g pcDNA3-IE2.

800

801 **Figure 4. IE1 knock-down attenuates HCMV-induced SOX2 down-regulation in NPCs.**

802 (A) IE1-directed knock-down efficiency of candidate shRNAs in HEL cells. HEL cells were
803 transduced with lentiviruses expressing shRNA-IE1-1 (sh-1), shRNA-IE1-2 (sh-2), shRNA-
804 IE1-3 (sh-3), or shRNA-scramble (scr). At 48 h post transduction, cells were infected with
805 HCMV (TNWT) at an MOI of 1 and collected at 24 or 48 hpi. IE1 protein levels were
806 determined by Western blotting. Actin served as a loading control. (B) IE1-directed knock-
807 down efficiency of sh-2 in HEL cells. HEL cells transduced with sh-2 or scr expressing
808 lentiviruses were infected with HCMV (TNWT) as in (A). Left: IE1 mRNA levels were
809 determined by qRT-PCR at the indicated times post infection; data from two independent
810 experiments were analyzed by one way ANOVA, and results are presented as average \pm SD.
811 *, $p \leq 0.05$; **, $p \leq 0.01$. Right: protein levels were determined accordingly at the indicated
812 times by Western blotting. (C) Effect of sh-2 on IE1 and SOX2 expression in NPCs. NPCs
813 were transduced with sh-2 or scr expressing lentiviruses, cultured for 48 h, reseeded at a
814 density of 3×10^6 cells/dish, and mock (M)- or virus (V)-infected with TNWT at an MOI of 1.
815 Protein levels of IE1, UL44, gB and SOX2 at the indicated times post infection are shown.
816 Actin served as a loading control.

817

818 **Figure 5. HCMV infection or IE1 expression inhibit STAT3 tyrosine phosphorylation**

819 **and promote nuclear accumulation of unphosphorylated STAT3 in NPCs.** (A) Inhibition

820 of STAT3 tyrosine (Y705) phosphorylation by HCMV infection. NPCs were mock (M)- or
821 virus (V)-infected with TNWT at an MOI of 3 and collected at the indicated times post
822 infection. The protein levels of IE1, pSTAT3 and total STAT3 were determined by Western
823 blotting. Actin served as a loading control. (B) Trapping STAT3 in nuclear by HCMV
824 infection. NPCs were mock (M)- or virus (V)-infected with TNWT at an MOI of 1. Left: For

825 indirect immunofluorescence analysis, NPCs on coverslips collected at 8 hpi were stained
826 with antibodies against STAT3 (green) or IE1/IE2 (red), and nuclei were counterstained with
827 Hoechst 33342 (blue). Infected (IE1/IE2 positive) cell is indicated with a white arrow. Scale
828 bar, 10 μ m. Right: For cellular fractionation analysis, fractions enriched in cytoplasmic (Cyt)
829 or nuclear (Nuc) proteins were prepared from cells collected at 4 or 8 hpi. Protein levels of
830 pSTAT3 and total STAT3 in each fraction were determined by Western blotting. GAPDH and
831 lamin B1 served as controls for the Cyt and Nuc fraction, respectively. (C, D and E) Inhibition
832 of tyrosine phosphorylation and nuclear sequestration of unphosphorylated STAT3 by IE1.
833 Fractions enriched in cytosolic (Cyt) or nuclear (Nuc) proteins or total cell extracts were
834 prepared. (C) For transient transfection analysis, NPCs were transfected with pcDNA3-IE1 or
835 empty vector (Ctrl). Protein levels of IE1, pSTAT3, and total STAT3 were determined by
836 Western blotting. GAPDH and lamin B1 served as controls for the Cyt and Nuc fraction,
837 respectively. For HCMV infection analysis, NPCs were mock-infected (M) or infected with
838 TNWT, TNdIE1, or TNrvIE1 viruses at an MOI of 10. The levels of the indicated viral and
839 cellular proteins in whole cell extracts (D, E) or in the Cyt and Nuc fractions (F) were
840 determined by Western blotting. Actin, GAPDH and lamin B1 served as controls for total
841 extracts or Cyt and Nuc fractions, respectively.

842

843 **Figure 6. SOX2 expression strictly depends on pSTAT3, and IE1 mediates SOX2**
844 **depletion by inhibiting STAT3 activation.** (A) Inhibition of STAT3 correlates with
845 suppression of SOX2 expression. NPCs were treated with the chemical inhibitor
846 cryptotanshinone (CTS) for the indicated times. The protein levels of total STAT3, pSTAT3,
847 and SOX2 were determined by Western blotting. Actin served as a loading control. Und,
848 undetectable. (B) Silencing of STAT3 correlates with suppression of SOX2 expression. NPCs
849 were transduced with lentiviruses Tet-pLKO-puro-shLuci (shLuci), Tet-pLKO-puro-shDsRed

850 (shDsRed), Tet-pLKO-puro-shSTAT3-1 (shSTAT3-1) or Tet-pLKO-puro-shSTAT3-2
851 (shSTAT3-2) and treated with doxycycline for 48 h to induce shRNA expression. The protein
852 levels of total STAT3, pSTAT3, and SOX2 were determined by Western blotting. Actin served
853 as a loading control. (C) IL-6-mediated activation STAT3 correlates with induction of SOX2
854 expression. NPCs were treated with IL-6 for 2 or 24 h. The protein levels of pSTAT3, total
855 STAT3 and SOX2 were monitored by Western blotting. Actin served as a loading control.
856 Data from three independent experiments were analyzed by one way ANOVA, and results are
857 presented as average \pm SD. *, $p \leq 0.05$; **, $p \leq 0.01$. (D) IL-6 counteracts IE1-dependent
858 SOX2 down-regulation in transiently transfected NPCs. NPCs were transfected with
859 pcDNA3-IE1, treated with IL-6 for 4 h or left untreated and collected at 48 h post
860 transfection. The protein levels of IE1, total STAT3, pSTAT3, and SOX2 were determined by
861 Western blotting. Actin served as a loading control. Data from three independent experiments
862 were analyzed by one way ANOVA, and results are presented as average \pm SD. *, $p \leq 0.05$;
863 **, $p \leq 0.01$. (E) IL-6 counteracts IE1-dependent SOX2 down-regulation in HCMV-infected
864 NPCs. NPCs were infected with TNWT or TNdlIE1 viruses at an MOI of 10, treated with IL-
865 6 for 4 h or left untreated, and collected at 48 hpi. The protein levels of IE1/IE2, total STAT3,
866 pSTAT3, and SOX2 were determined by Western blotting. Actin served as a loading control.
867 Data from three independent experiments were analyzed by one way ANOVA, and results are
868 presented as average \pm SD. *, $p \leq 0.05$; **, $p \leq 0.01$.
869

Table 1. Oligonucleotides used in this study.

Purpose	Name	Sequence (5'-3')
IE1 knock-do wn	scr F	CCGGCCTAAGGTTAAGTCGCCCTCGCTCGAGCGAGGGCGACTT AACCTTAGGTTTTTG
	scr R	AATTCAAAAACCTAAGGTTAAGTCGCCCTCGCTCGAGCGAGGG CGACTTAACCTTAGG
	sh-1 F	CCGGGCATGTATGAGAACTACATTGCTCGAGCAATGTAGTTCTC ATACATGCTTTTTG
	sh-1 R	AATTCAAAAAGCATGTATGAGAACTACATTGCTCGAGCAATGT AGTTCTCATACATGC
	sh-2 F	CCGGGCTGTGCTGCTATGTCTTAGACTCGAGTCTAAGACATAGC AGCACAGCTTTTTG
	sh-2 R	AATTCAAAAAGCTGTGCTGCTATGTCTTAGACTCGAGTCTAAGA CATAGCAGCACAGC
	sh-3 F	CCGGGCCTGAGGTTATCAGTGTAATCTCGAGATTACACTGATAA CCTCAGGCTTTTTG
	sh-3 R	AATTCAAAAAGCCTGAGGTTATCAGTGTAATCTCGAGATTACA CTGATAACCTCAGGC
STAT3 knock-do wn	#1102	CCGGGCCTCAAGATTGACCTAGACTCGAGTCTAGGTCAATCTTG AGGCTTTTT
	#1103	AATTAAAAAGCCTCAAGATTGACCTAGACTCGAGTCTAGGTCA ATCTTGAGGC
	#1134	CCGGAGTCAGGTTGCTGGTCAAACCTCGAGTTTGACCAGCAACC TGACTTTTTT
	#1135	AATTAAAAAGTCAGGTTGCTGGTCAAACCTCGAGTTTGACCAG CAACCTGACT
	#1098	CCGGGTGCGTTGCTAGTACCAACCTCGAGGTTGGTACTAGCAA CGCACTTTTT
	#1099	AATTAAAAAGTGCGTTGCTAGTACCAACCTCGAGGTTGGTACT AGCAACGCAC
	#1138	CCGGGTGGGAGCGCGTGATGAACCTCGAGGTTTCATCACGCGCT CCCCTTTTT
	#1139	AATTAAAAAGTGGGAGCGCGTGATGAACCTCGAGGTTTCATCAC GCGCTCCAC
PCR	pp65 F	CGCGGATCCATGGAGTCGCGCGGTCCCGT
	pp65 R	CCGGAATTCTCAACCTCGGTGCTTTTTGGG
qRT-PC R	SOX2 F	GCCGAGTGGAACCTTTTGTCG
	SOX2 R	GCAGCGTGTACTTATCCTTCTT
	GAPDH F	GAGTCAACGGATTTGGTCGT
	GAPDH R	GACAAGCTTCCCCTTCTCAG

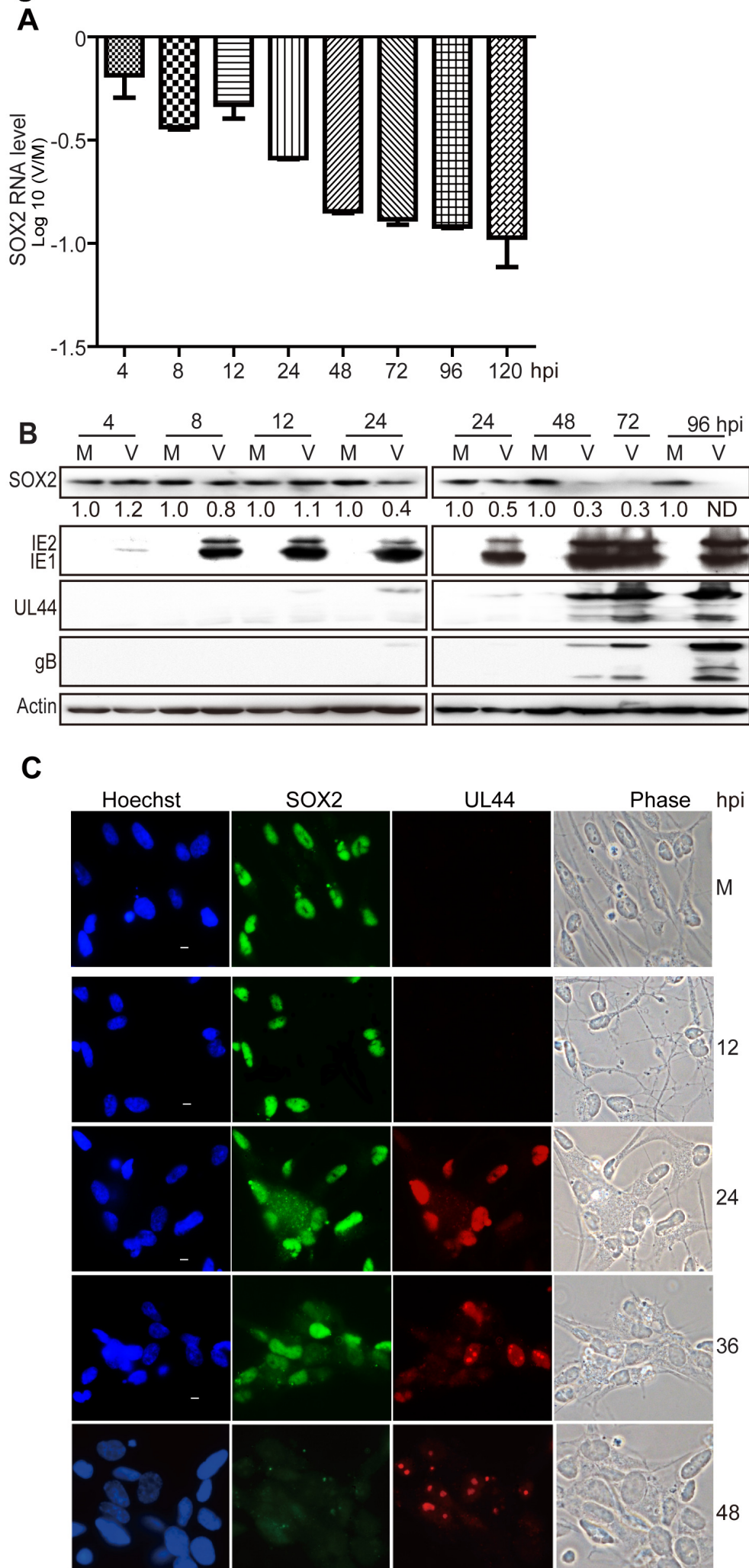
Figure 1

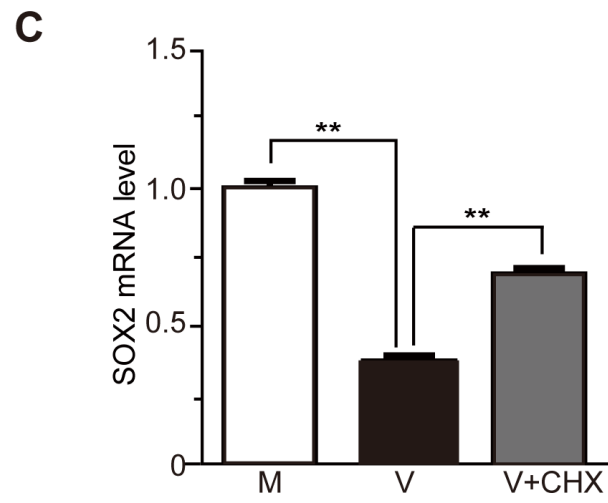
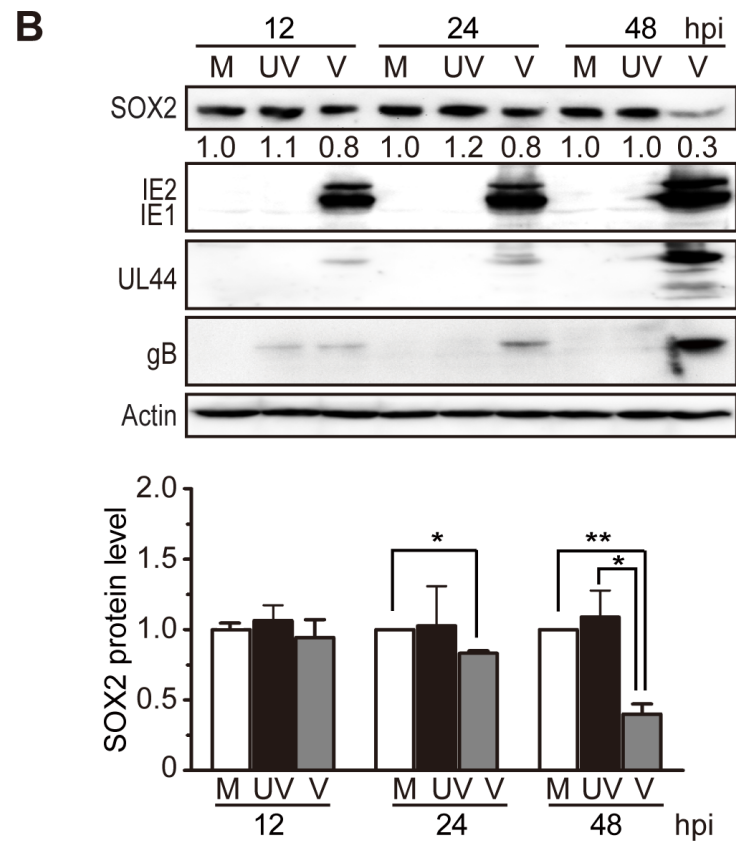
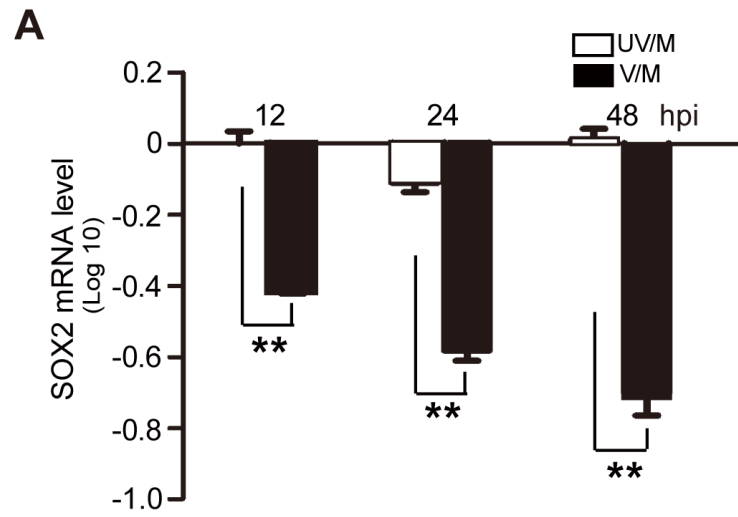
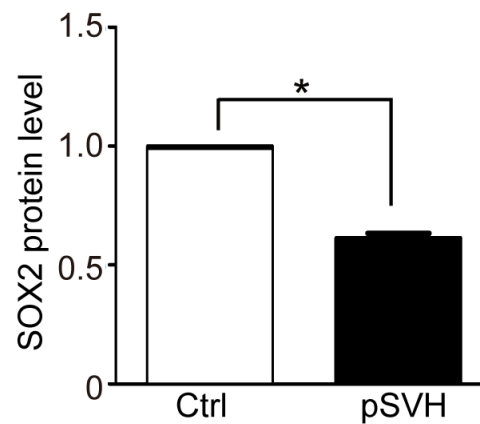
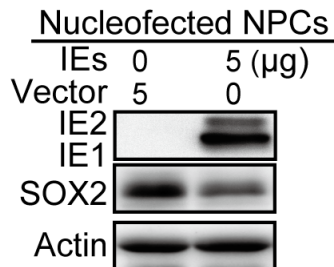
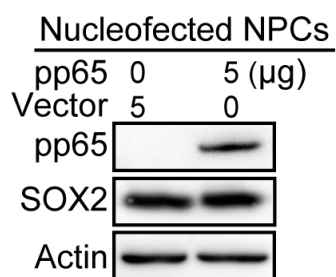
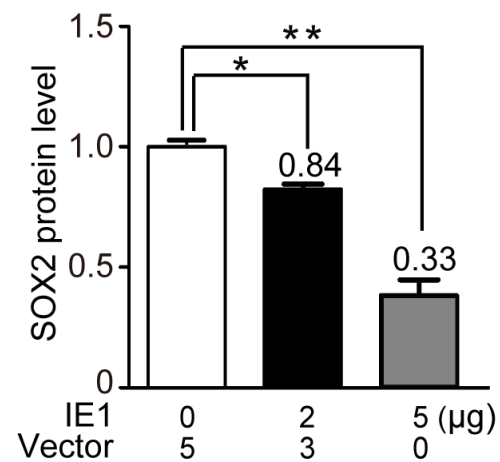
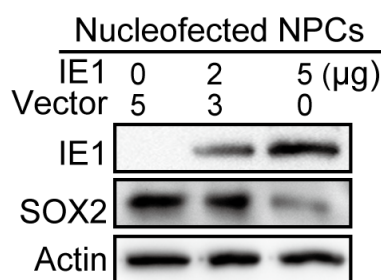
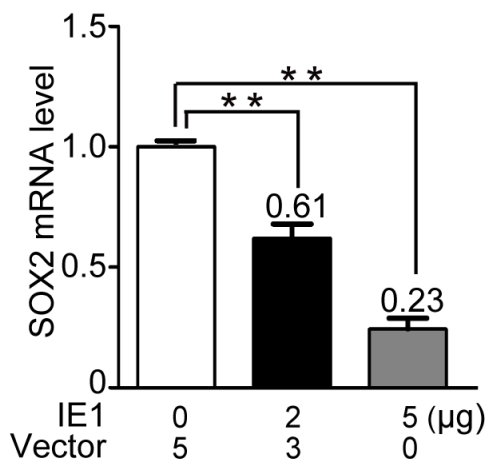
Figure 2

Figure 3

A



B



C

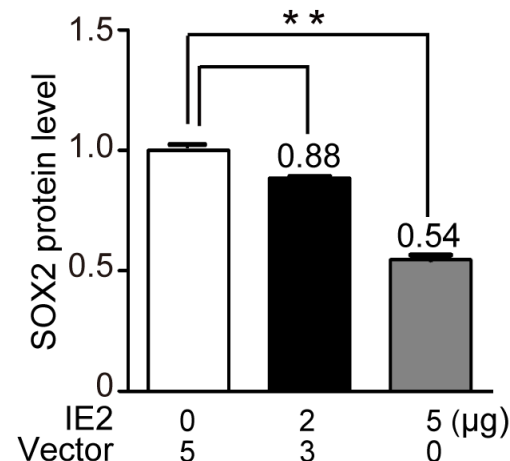
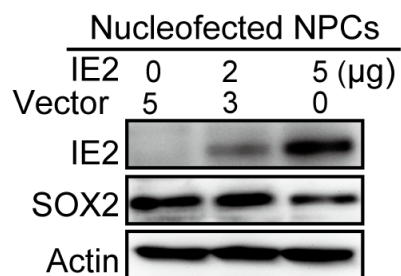
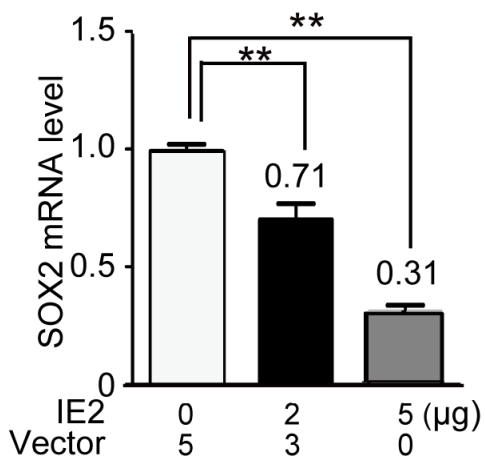
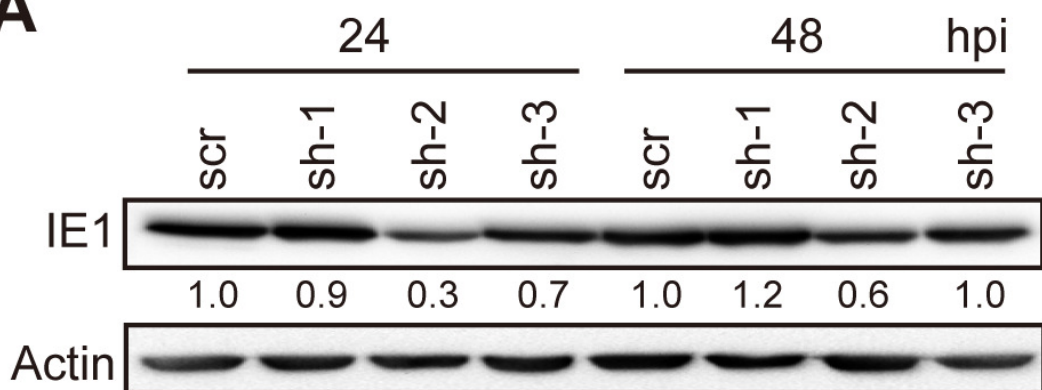
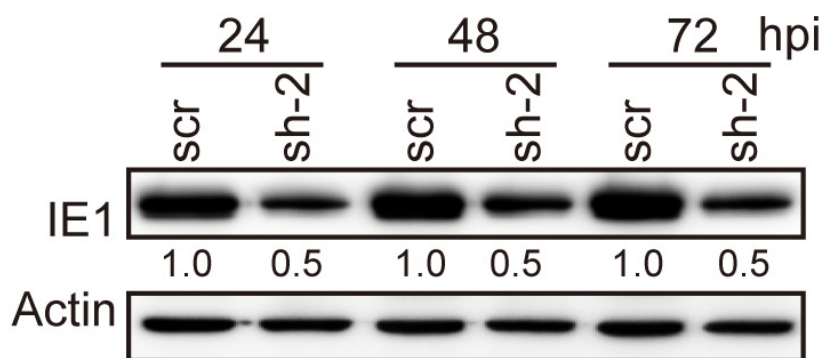
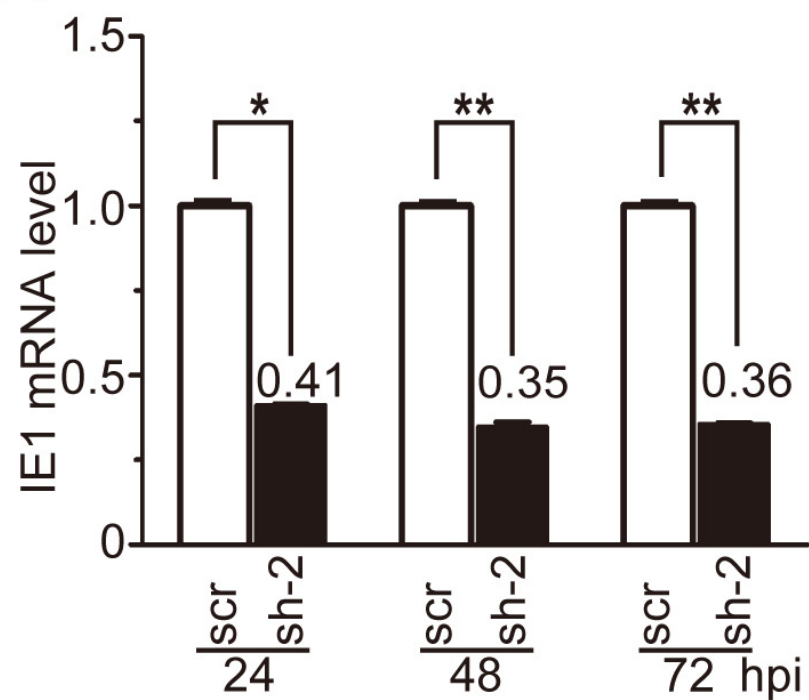


Figure 4

A



B



C

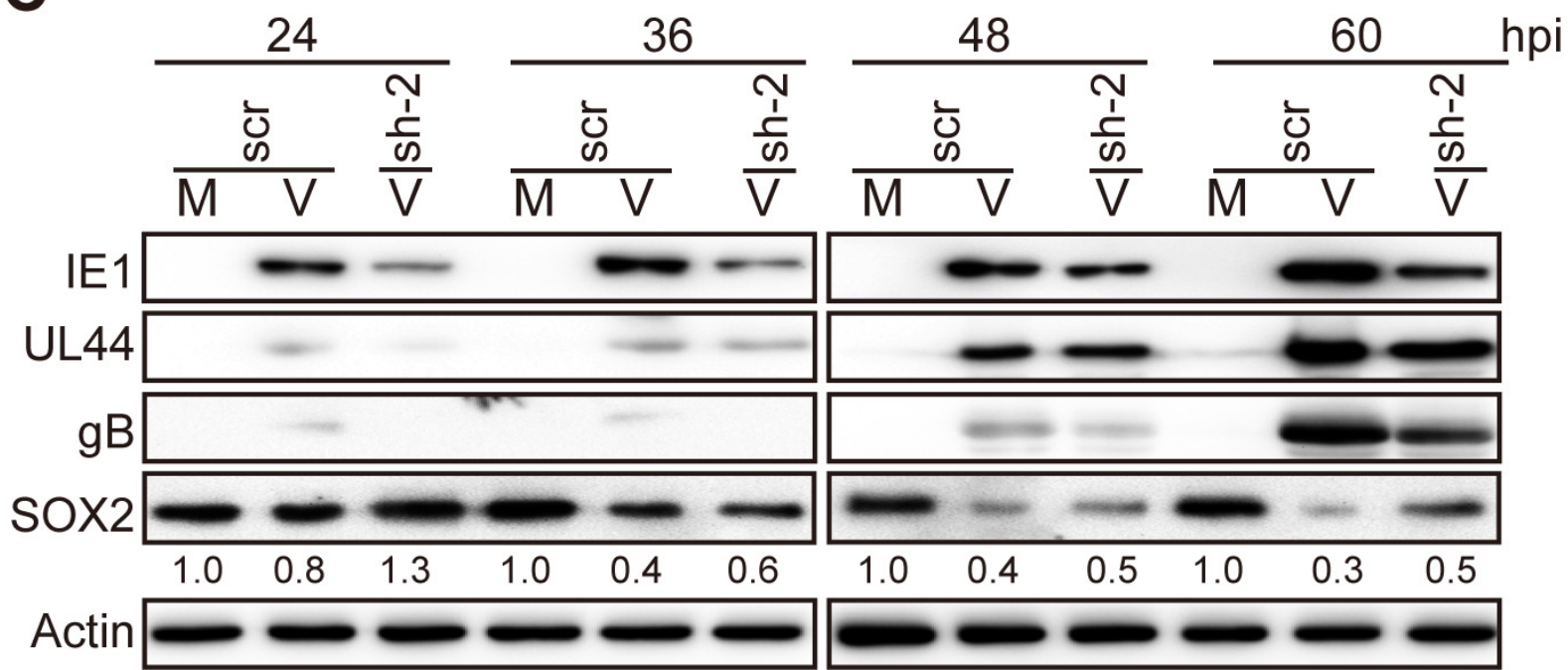


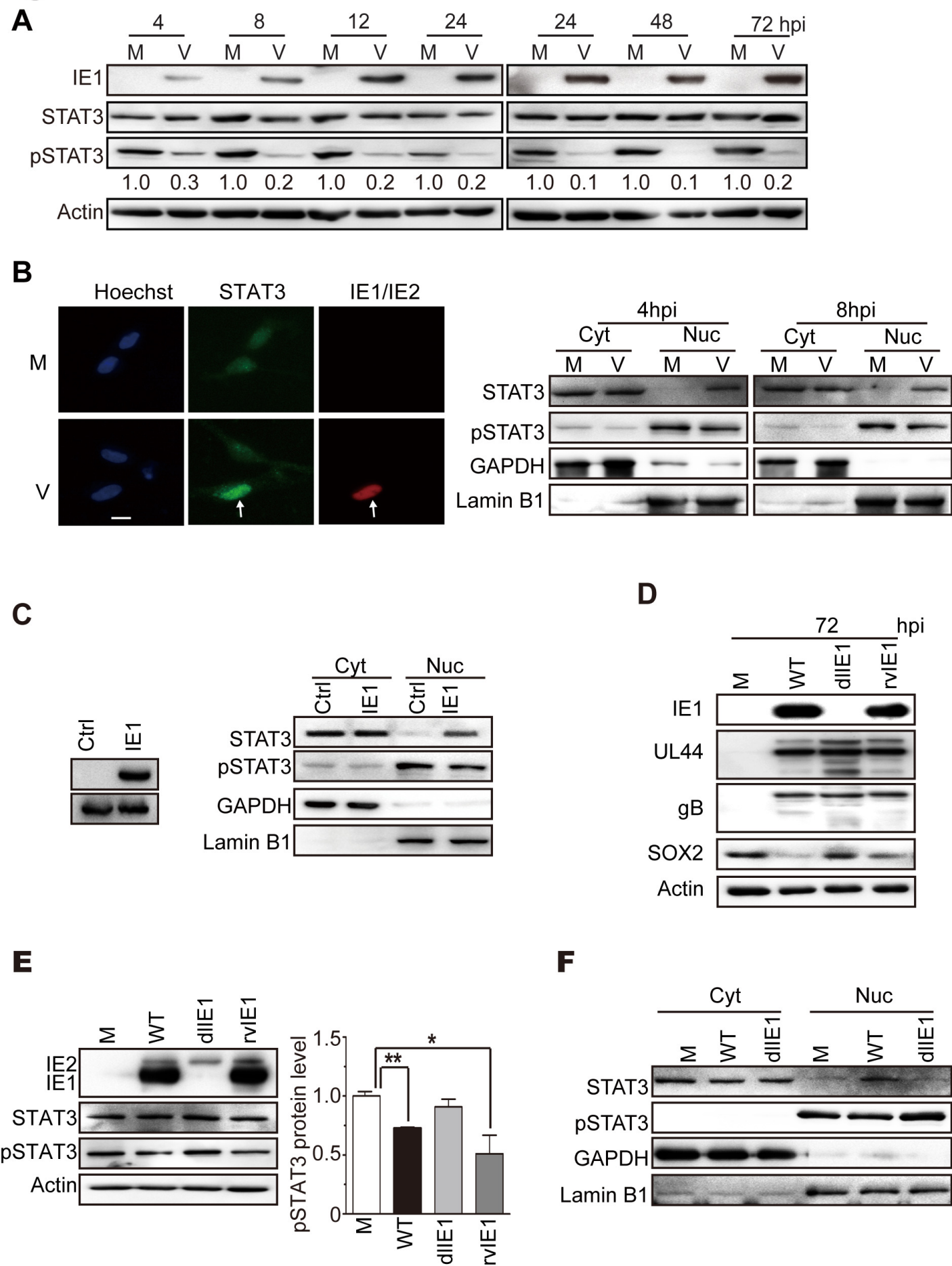
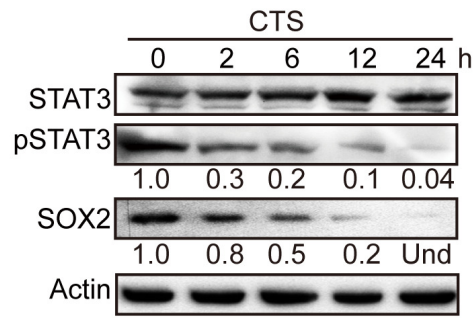
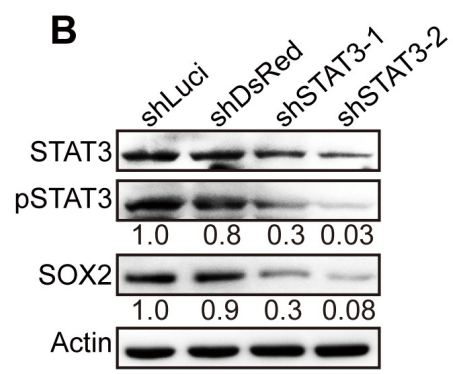
Figure 5

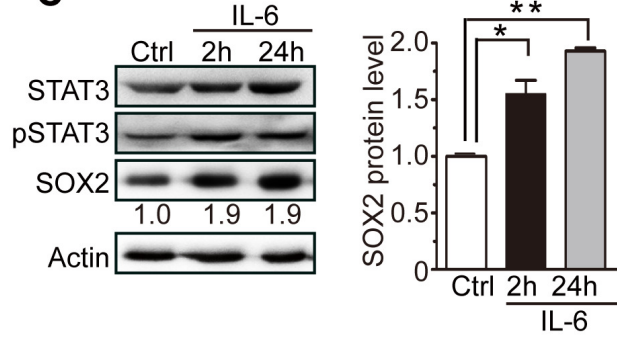
Figure 6 A



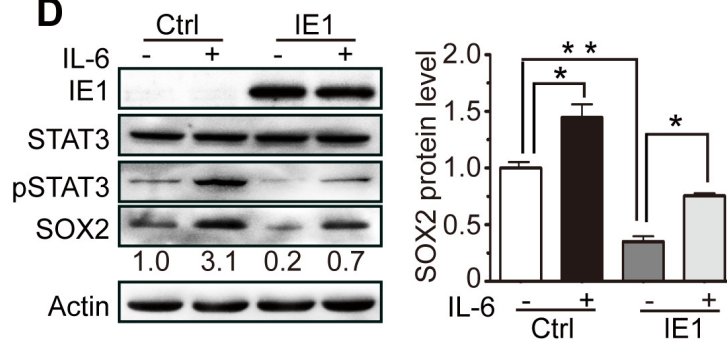
B



C



D



E

